



Universiteit
Leiden

The Netherlands

Exploring the *Mycobacterium tuberculosis* antigenome: New insights for the development of vaccines, diagnostics and drugs

Coppola, M.

Citation

Coppola, M. (2022, November 3). *Exploring the Mycobacterium tuberculosis antigenome: New insights for the development of vaccines, diagnostics and drugs*. Retrieved from <https://hdl.handle.net/1887/3485193>

Version: Publisher's Version

License: [Licence agreement concerning inclusion of doctoral thesis in the Institutional Repository of the University of Leiden](#)

Downloaded from: <https://hdl.handle.net/1887/3485193>

Note: To cite this publication please use the final published version (if applicable).



CHAPTER 2

New genome-wide algorithm identifies novel *in vivo* expressed *Mycobacterium tuberculosis* antigens inducing human T-cell responses with classical and unconventional cytokine profiles

Mariateresa Coppola¹, Krista E van Meijgaarden¹, Kees LMC Franken¹, Susanna Commandeur^{1,#a}, Gregory Dolganov², Igor Kramnik³, Gary K Schoolnik², Inaki Comas^{4,5}, Ole Lund⁶, Corine Prins¹, Susan JF van den Eeden¹, Gro E Korsvold⁷, Fredrik Oftung⁷, Annemieke Geluk^{1¶} and Tom HM Ottenhoff^{1¶}

¹ Department of Infectious Diseases, Leiden University Medical Center, Leiden, The Netherlands;

² Department Microbiology Immunology, Stanford Univ. School of Medicine, Stanford, USA;

³ Department Immunology Infectious Diseases, Harvard School of Public Health, Boston, USA;

⁴ Institute of Biomedicine of Valencia (IBV-CSIC) Valencia, Spain;

⁵ CIBER in Epidemiology and Public Health, Madrid, Spain;

⁶ Dept. Systems Biology, Technical Univ. Denmark;

⁷ Department of Infectious Disease Immunology, Domain for Infection Control and Environmental Health, Norwegian Institute of Public Health, Oslo, Norway.

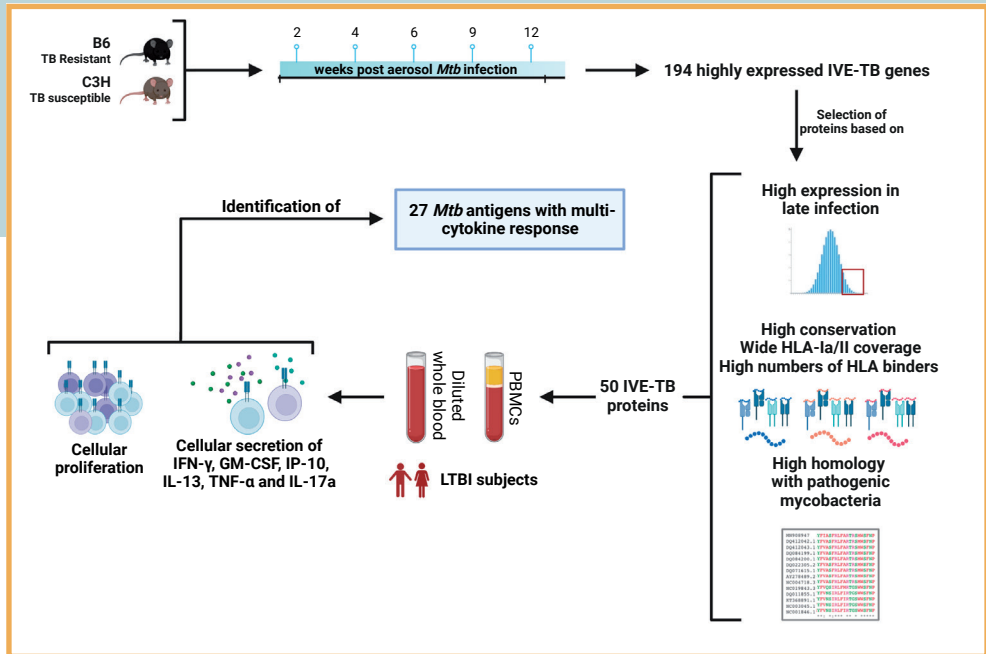
^{#a}: Current Address: Dept. of Medical Microbiology and Infection Control, VU University Medical Center, Amsterdam, The Netherlands

[¶]: These authors are joint senior authors

Sci Rep. 2016 Nov 28; 6:37793

doi: 10.1038/srep37793

ABSTRACT



New strategies are needed to develop better tools to control TB, including identification of novel antigens for vaccination. Such *Mtb* antigens must be expressed during *Mtb* infection in the major target organ, the lung, and must be capable of eliciting human immune responses. Using genome-wide transcriptomics of *Mtb* infected lungs we developed data sets and methods to identify IVE-TB (*in vivo* expressed *Mtb*) antigens expressed in the lung. Quantitative expression analysis of 2,068 *Mtb* genes from the predicted first operons identified the most upregulated IVE-TB genes during *in vivo* pulmonary infection. By further analysing high-level conservation among whole-genome sequenced *Mtb*-complex strains ($n=219$) and algorithms predicting HLA-class-Ia and II presented epitopes, we selected the most promising IVE-TB candidate antigens. Several of these were recognized by T-cells from *in vitro* *Mtb*-PPD and ESAT6/CFP10-positive donors by proliferation and multi-cytokine production. This was validated in an independent cohort of latently *Mtb*-infected individuals. Significant T-cell responses were observed in the absence of IFN- γ -production. Collectively, the results underscore the power of our novel antigen discovery approach in identifying *Mtb* antigens, including those that induce unconventional T-cell responses, which may provide important novel tools for TB vaccination and biomarker profiling. Our generic approach is applicable to other infectious diseases.

INTRODUCTION

Since WHO in 1993 declared tuberculosis (TB) a global public health emergency, 22 million lives have been saved and 56 million patients have been adequately treated (1). Despite these encouraging achievements, it will not be possible to eradicate TB solely by conventional strategies. Recent modelling studies (2) show that the current decline in TB incidence needs to be accelerated significantly, which cannot be achieved without developing and implementing novel tools. The increase in multidrug-resistance incidence (3), the association with HIV-infection and non-communicable diseases (4), the lack of an efficient vaccine and the difficulty in timely diagnosing TB (5) represent just a few of the challenges that need to be addressed. Improved diagnostics (6), safer and more accessible treatments for active and latent *Mycobacterium tuberculosis* (*Mtb*) infection (7) and new effective pre- and post-exposure vaccines must all be developed before we can reach TB elimination (8, 9).

Sixteen TB vaccine candidates are currently in various phases of clinical testing (10). The majority of these candidates are subunit vaccines which mainly contain combinations of a limited number of antigens identified mostly under *in vitro* culture conditions, thereby representing less than one percent of the targetable ~ 4,000 proteins encoded by *Mtb* genome (11). So far, in humans, none of these vaccines has shown to confer protection superior to Bacillus Calmette-Guérin (BCG), the only licensed TB vaccine available. Intradermal BCG administration by itself, however, does not induce protection against TB consistently (12, 13). Recently, MVA85A, the first single antigen-based TB vaccine candidate tested in an efficacy phase IIb trial, failed to boost protection against TB in BCG-vaccinated infants (14). Following this disappointing outcome, the field has been reconsidering the design of future TB vaccines (15), including new efforts towards better rationalized and comprehensive antigen selection approaches, both in pre-clinical (16) and clinical studies (17-20).

To identify new *Mtb* antigens, we have hypothesized it is important to consider host-pathogen interactions in antigen discovery, rather than focusing on the pathogen alone. We have proposed to define the *Mtb* antigen repertoire expressed *in vivo* during pulmonary infection. The lung is the primary organ in which *Mtb* resides and interacts with the human immune system (9, 11, 21, 22), and where it initiates the process of infection and pathogenesis, setting the stage for future transmission. In our previous preliminary study (23), we have explored gene expression profiles during pulmonary infection in mice with varying susceptibility to TB. In combination with the *in vitro* immune characterization of human cells from *Mtb* exposed individuals, this work allowed us to identify the first *in vivo* expressed TB candidate antigens (IVE-TB). This included Rv2034, which induced poly-functional T cell responses with

Mtb-inhibitory activity at the clonal level (24) and induced encouraging protection against TB challenge in HLA-DR transgenic mice and in guinea pigs (25). Several other strategies have been followed to explore the *Mtb* anti-genome (11), including predictive MHC-peptide binding bioinformatics tools combined with human- or mouse-based T-cell screening approaches to discover novel HLA-class Ia (11, 26), Ib (27) and II (11, 19, 28, 29) restricted *Mtb* antigens.

In this study, we have used genome-wide transcriptomics of *Mtb* from the lungs of infected mice, and developed extensive data sets and methods to identify promising pulmonary IVE-TB antigens. We generated a novel *Mtb* gene expression database from isolated *Mtb* RNA from the lungs of large numbers of susceptible (C3HeB/FeJ) and resistant (C57BL/6J) mice after aerosol *Mtb* (Erdman) infection, and analysed the expression of 2,068 *Mtb* genes to allow the selection of the most upregulated IVE-TB genes during early and late phase infection. By combining these data with extended analysis of high-level genetic conservation in a set of 219 whole-genome sequenced *Mtb* complex strains (30), and with the presence of HLA class Ia and II peptide binding motifs as well as homology with other pathogenic mycobacteria, new IVE-TB candidate antigens could be selected. Several of these antigens were recognized by T-cells from *in vitro* *Mtb* responsive donors and latently *Mtb*-infected donors as measured by proliferation and multi-cytokine production, including antigens that induced responses other than IFN- γ . Collectively, these results underscore the power of our novel antigen discovery approach in identifying new *Mtb* antigens which may provide important tools for TB vaccination and biomarker profiling studies.

RESULTS

Identification of novel *in vivo* expressed *Mtb* (IVE-TB) genes upregulated during pulmonary *Mtb* infection

To discover antigens able to elicit cellular immune responses against *Mtb* proteins highly expressed in the lung, we investigated the *in vivo* expression profile of 2,068 *Mtb* genes (IVE-TB) based on *Mtb* RNA isolated from murine infected pulmonary tissue. IVE-TB qRT-PCR-based gene expression data sets were obtained from groups of four mice per strain, characterized by high vs. low susceptibility to tuberculosis (C3HeB/FeJ vs. C57BL/6J), at five time points (Figure 1A) after aerosol *Mtb* Erdman infection. Data were normalized to standard reference gene copy numbers (RGCNs). IVE-TB genes with the highest and most persistent RGCNs were selected (top 15% expressed genes in all 10 data sets), independently of host background or infection phase, resulting in 194 candidates (Figure 1A; Supplementary Table 1). The proportional distribution of the functional categories among these 194 IVE-TB

genes was compared to that of the whole *Mtb* genome. The categories *intermediary metabolism and respiration, regulatory protein, cell wall and cell processes, information pathways, lipid metabolism*, were over-represented among the IVE-TB genes; while the categories *virulence, detoxification, adaptation, PE/PPE, conserved hypotheticals and insertion seqs and phages* were under-represented (Supplementary Figure 1).

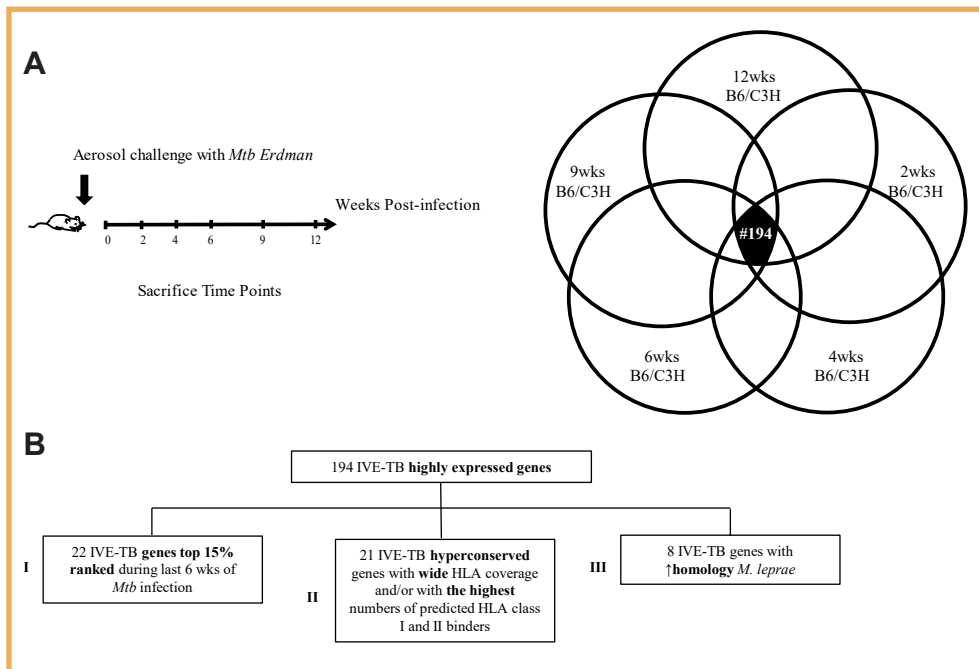


Figure 1. Gene expression analysis of IVE-TB genes during pulmonary infection and *In vivo* expressed *Mtb* (IVE-TB) gene selection algorithm. (A) The time line represents the timescale used to challenge and sacrifice at two, four, six, nine and twelve weeks (wks) TB resistant (B6) and susceptible (C3H) mice ($n=$ four per group). For each time point, *Mtb* RNA was isolated from the lung of *Mtb*-infected mice and the expression of 2,068 *Mtb* RGCNs was analysed. The most consistently upregulated IVE-TB genes ($n=194$) during early and late phase murine pulmonary *Mtb* infection were selected independently from the host background. Each circle corresponds to the top 15% highest expressed *Mtb* genes per mouse strain and time point of *Mtb* infection. The overlapping area in black represents the 194 overlapping IVE-TB genes common to all conditions. (B) The flow chart shows the analyses performed to determine the most promising *in vivo* expressed (IVE-TB) *Mtb* antigens candidates from the 194 IVE-TB genes selected according to their high expression during murine pulmonary *Mtb* infection. Four subgroups were selected combining different parameters: (I) gene expression during last 6 weeks (wks) of *Mtb* infection; (II) conservation, wide HLA class Ia and II alleles coverage and/or the highest number of HLA-peptide binding motifs for HLA class I and II; (III) high homology with *M. leprae*. Genes that could not be expressed as recombinant proteins were excluded.

Conservation and *in silico* predicted antigenicity of the top up-regulated IVE-TB genes

To select IVE-TB candidates for immunogenicity testing in humans, we characterised the most up-regulated 194 IVE-TB genes for: their level of conservation among 219 *Mtb* whole-genome sequences; for their homology with BCG and other pathogenic mycobacteria; and for their *in silico* predicted antigenicity.

First, all 194 selected IVE-TB genes were screened for their amino acid (aa) sequence homology with 219 whole-genome sequenced *Mtb* complex strains isolated from clinical specimens as described (30). Considering the number of non-synonymous aa changes for each protein weighted for the number of aa, 154 genes were found to be highly conserved (aa conservation $\geq 98\%$) among all seven *Mtb* lineages (Supplementary Table 2 available online at: https://static-content.springer.com/esm/art%3A10.1038%2Fsrep37793/MediaObjects/41598_2016_BFsrep37793_MOESM1_ESM.pdf). Further BLASTp analysis showed that most of the IVE-TB protein sequences were highly homologous to proteins present in BCG and other pathogenic (*M. leprae*, *M. ulcerans*) or atypical mycobacteria (*M. kansasii*) (NTM) (Supplementary Table 3 available online at: https://static-content.springer.com/esm/art%3A10.1038%2Fsrep37793/MediaObjects/41598_2016_BFsrep37793_MOESM1_ESM.pdf). This observation suggests that the majority of IVE-TB genes potentially could boost specific immune responses induced by previous BCG vaccination or by NTM exposure. Secondly, since classical HLA-restricted T-cell responses are required for protection against TB, two *in silico* tools, NetMHCcons 1.031 and NetMHCIIpan 3.032, were used to predict HLA class Ia and class II binding epitopes, respectively, in the 194 IVE-TB gene-encoded proteins. This query provided both quantitative and qualitative data, i.e., the absolute number of predicted peptide binding motifs for any HLA class Ia or class II molecule as well as the HLA class Ia and class II alleles predicted to bind epitopes from the proteins, respectively (Supplementary Table 2 available online at: https://static-content.springer.com/esm/art%3A10.1038%2Fsrep37793/MediaObjects/41598_2016_BFsrep37793_MOESM1_ESM.pdf). The HLA alleles included in this analysis should provide a large global coverage of the human HLA class Ia and II polymorphisms [virtually 98% for HLA class Ia33 and approximately 50-75% for HLA class II (34)].

Selection of candidate IVE-TB genes for immunogenicity testing on human cells

We next combined the *in vivo* expression data with the *in silico* analysis to identify the most promising IVE-TB candidate antigens among the 194 upregulated IVE-TB genes (Figure 1B, Supplementary Table 4 available online at: https://static-content.springer.com/esm/art%3A10.1038%2Fsrep37793/MediaObjects/41598_2016_BFsrep37793_

MOESM1_ESM.pdf). The first selected genes (n=22) (subgroup I) were those that ranked as top 15% IVE-TB genes during the later time points of *Mtb* infection (six wks), since we hypothesised this to be an important parameter in selecting antigens for driving T-cell responses against *Mtb* in the infected lung. The second selection (n=21) (subgroup II) included hyperconserved IVE-TB genes with wide HLA class Ia and class II allele coverage and/ or with the highest number of peptide epitopes predicted to bind to HLA class Ia and HLA class II. The last group (n=eight) (subgroup III) of IVE-TB genes consisted of *Mtb* genes with high homology to *M. leprae* (genes taxid: 1769) (Rv0468, Rv0470c, Rv0501, Rv0640, Rv1390, Rv1846, Rv1872 and Rv2215). The rationale behind the last selection was to include candidates with potential cross-protection against *M. leprae* infection (35, 36). In addition, since these genes are conserved in *M. leprae*, which has strongly downsized its genome size compared to other pathogenic mycobacteria, these *M. leprae* genes could play important roles in intracellular mycobacterial survival (37). One gene (Rv0287) overlapped between two subgroups (I and II). In view of high-throughput recombinant protein production, some genes, although matching the criteria of inclusion, had to be excluded based on aa length and/or predicted transmembrane regions and hydrophobicity, leading to expression and solubility issues. Two additional genes (Rv1197 and Rv1805) (from subgroups I and II) were deselected due to the low yields obtained during recombinant protein production (Supplementary Table 4 available online at: https://static-content.springer.com/esm/art%3A10.1038%2Fsrep37793/MediaObjects/41598_2016_BFsrep37793_MOESM1_ESM.pdf). Combining all three subgroups, a total of 50 genes was selected for further evaluation.

The most represented functions of the 50 IVE-TB genes were in line with the categories over-represented in the 194 IVE-TB genes compared to the whole *Mtb* genome. Some of the 50 IVE-TB genes selected here have already been described as T cell antigens and have been formulated as TB vaccines currently in clinical trials (20, 29, 38-40) or pre-clinical studies (16, 23, 26, 28, 41, 42) (Table 1). Those consistent findings strongly validate our antigen discovery algorithm. For comparative purposes, the known antigens matching our selection procedure were included in the immunogenicity study below. ESAT6 was part of the 50 IVE-TB genes fulfilling the inclusion criteria and was produced as fusion protein dimerized to CFP10 (E/C), since this is known to enhance its discriminatory TB diagnostic value (6, 43). Another five *esx* genes qualifying as IVE-TB were also formulated as heterodimers with their co-expressed partner proteins. The two IVE-TB gene pairs Rv0287/Rv0288 and Rv2346/Rv2347 were produced as fusion proteins (Rv0287/88 and Rv2346/47). Rv3615 was produced and tested as single protein as well as heterodimer with Rv3614 (although Rv3614 was not in the IVE-TB gene selection). Taken together, 49 recombinant proteins were produced for antigenicity testing. Since E/C was used as a diagnostic

to distinguish previous exposure to *Mtb* we analysed this fusion protein separately, such that in the paragraphs below we refer to a total of 48 IVE-TB proteins.

Recognition of the novel IVE-TB antigens by human T cell proliferation

As a first step in evaluating the newly selected IVE-TB proteins (n=48), we tested their immunogenicity using PBMCs from individuals with or without pre-existing immune response to mycobacteria (n=19). Based on their *in vitro* proliferative responses

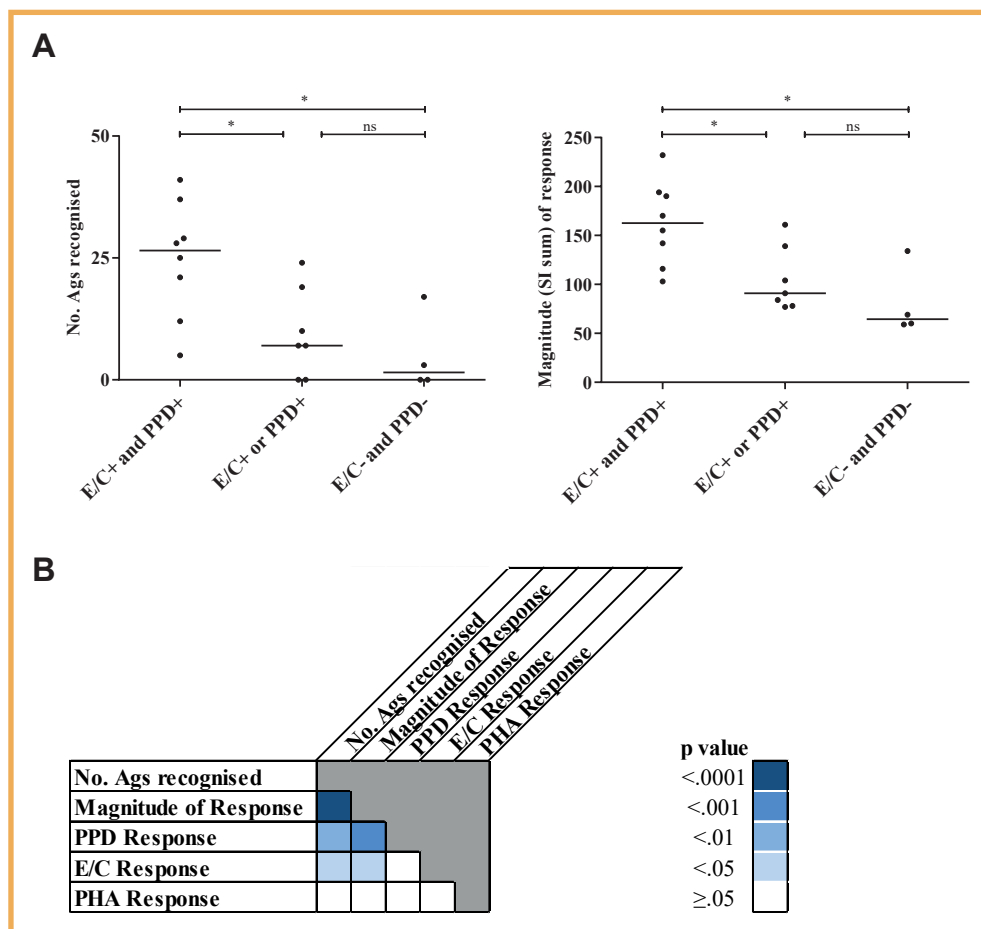


Figure 2. Lymphocyte proliferative responses to IVE-TB proteins in individuals with different exposures to *Mtb*. (A) Donors (n=19) were divided into three groups based on their lymphocyte proliferative response to *Mtb* ESAT6/CFP10 (E/C) or PPD. The total number of antigens recognized (left) and the overall magnitude of responses generated (right) after stimulation are indicated per individual as a closed circle (●). (B) Donors were ranked according to the lymphocyte proliferation responses to PHA, PPD, E/C, the total proliferation, and the number of antigens recognized. The correlation among these variables was measured by Spearman r , and the statistical significance was expressed by two-tailed p -value.

to *Mtb* ESAT6/CFP10 (E/C) and *Mtb* purified protein derivative (PPD), donors were divided into three subgroups: double responders (E/C+ and PPD+), single responders (E/C+ or PPD+) and non-responders (E/C- and PPD-) to *Mtb*. The double responders recognized many antigens (range=5–41 out of the 48 selected antigens) in contrast to single responders (range=0–24 antigens) or non-responders (range=0–17 antigens) (Figure 2A) ($p=0.02$). A similar trend was observed for the magnitude of the proliferative response to the antigens: when expressed as stimulation index (SI), values ranged from 103 to 232 in the double responders, from 77 to 161 in the single responders and from 59 to 134 in the non-responders (Figure 2A) ($p=0.02$). Interestingly, the number of antigens recognized and the magnitude of response produced by each donor were strongly correlated (Spearman correlation: $r=0.96$; $p<0.0001$) (Figure 2B) indicating both high immunogenicity and immunodominance. The significantly greater T-cell proliferation observed in the double responders compared to the single or non-responder groups correlated with the presence of *Mtb* orthologues in NTM or BCG. We have previously reported that more than 50% of healthy donors from our Northern EU, non-endemic area responded to PPD (23, 41). This is further supported here by the strong correlation observed between the magnitude of the response to known mycobacterial stimuli (PPD, E/C) and the magnitude of response to the IVE-TB antigens (PPD: Spearman correlation $r=0.72$, $p<0.001$; E/C: Spearman correlation $r=0.48$, $p<0.05$) as well as the number of IVE-TB antigens recognized in relation to the donors *Mtb* responder status (PPD: Spearman correlation $r=0.64$, $p<0.01$; E/C: Spearman correlation $r=0.53$, $p<0.05$) (Figure 2B).

Next, we compared the relative immunodominance and the immunogenicity of the 48 IVE-TB antigens and controls (E/C, PPD, and PHA) based on SI values measured in the single (E/C+ or PPD+) and double (E/C+ and PPD+) responders ($n=15$). By ranking the antigens according to the number of positive responses (immunodominance) and the magnitude of proliferation elicited by each antigen for all donors (immunogenicity), we found that these parameters correlated well (Spearman correlation $r=0.93$, $p<0.0001$). Using this distribution, it was possible to identify a group of 16 from the top 20 antigens significantly concordant for both variables. Their functions did not only fall into categories overrepresented among the 194 IVE-TB genes (*intermediary metabolism and respiration, cell wall and cell process, information pathways and lipid metabolism*), but also in one underrepresented category (*virulence, detoxification and adaptation*) (Figure 3).

In summary, these results show that from the 48 tested IVE-TB proteins, 16 were frequently and highly recognized by the PBMCs from donors with recall responses to mycobacteria as indicated by *Mtb* specific T cell proliferation.

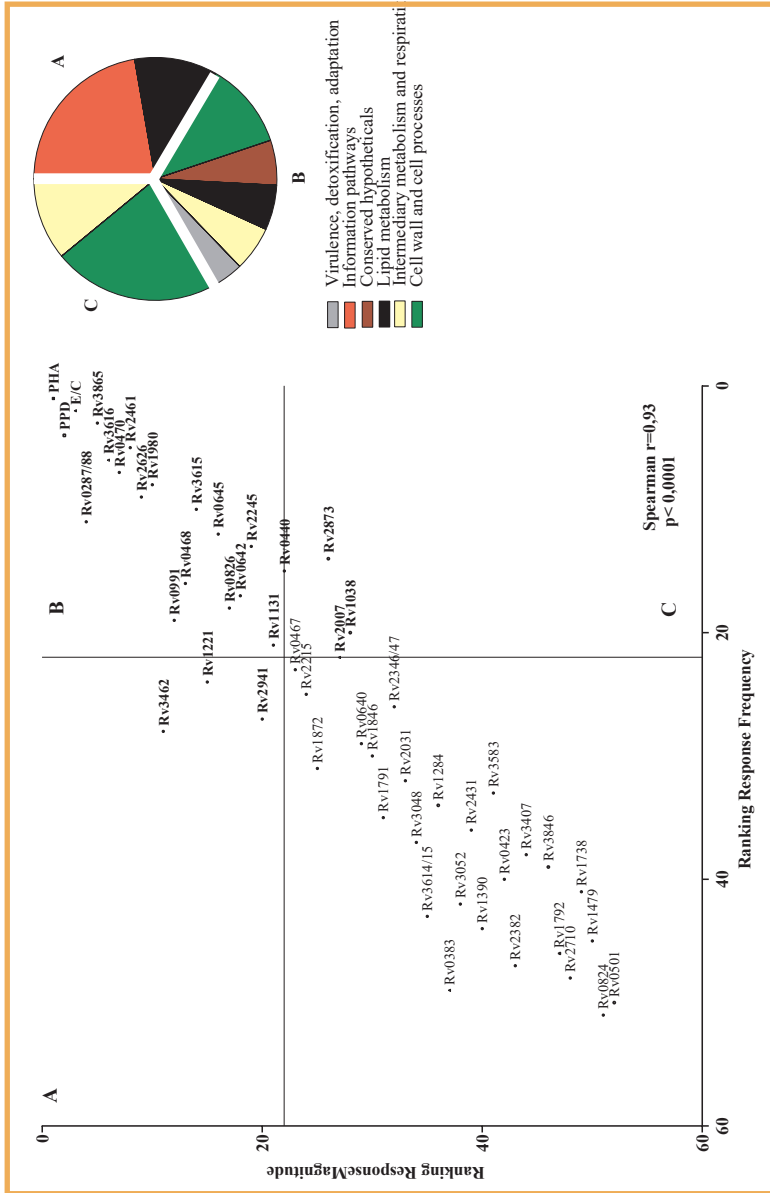


Figure 3. Immunodominance and immunogenicity of IVE-TB antigens based on lymphocyte proliferative responses. The immunodominance (x-axis) and immunogenicity (y-axis) of the new IVE-TB antigens (Ags), based on antigen-specific T cell proliferation measured in the single (E/C+ or PPD+) and double (E/C+ and PPD+) responders (n=15), were compared. The correlation was determined by Spearman r , and the statistical significance was calculated as a two-tailed p-value. In quadrant A are the top immunogenic antigens, in quadrant B the top frequently recognized antigens, and in quadrant C the top antigens for both parameters. The pie chart shows the distribution of the functional categories for each quadrant of the graph.

Cytokine responses to the new IVE-TB antigens induced from PBMC of *Mtb*-ESAT6/CFP10 and/or PPD *in vitro* responders

Next, to investigate the immunogenicity in more depth and characterize the type of T cell responses involved, we evaluated the induction of cytokines triggered by the IVE-TB proteins (n=48) in the same donors (n=12) evaluated in the above proliferation assays. PBMCs were stimulated with each IVE-TB antigen, E/C, PPD or PHA for six days and culture supernatants were tested for the presence of IFN- γ , IP-10, TNF- α , IL-17, IL-13, IL-10 and GM-CSF using a seven-plex assay. IL-10 was excluded from further analysis due to the low concentrations measured in response to antigens and PHA.

First, we analysed the number of individuals responding to the IVE-TB antigens based on the induced levels of the different cytokines. As in our previous report, we used IFN- γ concentrations ≥ 100 pg/ml in response to PPD and E/C, to discriminate individuals previously exposed to NTM or *Mtb* respectively; according to this criterion, donors were subsequently again divided into three groups: E/C+ PPD+, E/C- PPD+, and E/C- PPD-. As already described elsewhere (44-46), IFN- γ secretion did not always correlate with proliferative activity, suggesting that alternative cytokine responses might be involved. Half of the E/C+ PPD+ donors produced at least two different cytokines in response to 27 out of 48 IVE-TB proteins. Thirteen out of these 27 IVE-TB antigens induced increased levels of not only IFN- γ and IP-10 but also of TNF- α , IL-17 and IL-13. In the E/C- PPD+ group, higher levels of at least two different cytokines were induced by 15 IVE-TB antigens, which overlapped with those described for the E/C+ PPD+ group, although with a slightly different cytokine pattern than the double positive responders. In fact, TNF- α , IL-17, and IL-13 were induced with lower frequencies in the E/C- PPD+ group, while GM-CSF was induced with higher frequencies by three antigens (Rv1221, Rv1980 and Rv3616c). In the E/C- PPD- group, double cytokine induction was observed for only two out of the 27 antigens (Rv3615, and Rv2007) (Figure 4).

Subsequently, for each analyte the frequency and the magnitude of IVE-TB antigen induced responses were ranked to establish relative immunodominance and immunogenicity based on cytokine profiles. A significant correlation between these parameters was found for all cytokines analysed (Spearman correlation with $p < 0.0001$ for: $r_{\text{IFN-}\gamma} = 0.80$, $r_{\text{IP-10}} = 0.74$, $r_{\text{TNF-}\alpha} = 0.89$, $r_{\text{IL-17}} = 0.86$, $r_{\text{IL-13}} = 0.87$, $r_{\text{GM-CSF}} = 0.74$) (Figure 5A and Supplementary Figure 2).

Of note, several IVE-TB antigens were found to be both immunogenic and immunodominant for most cytokines considered (Figure 5B).

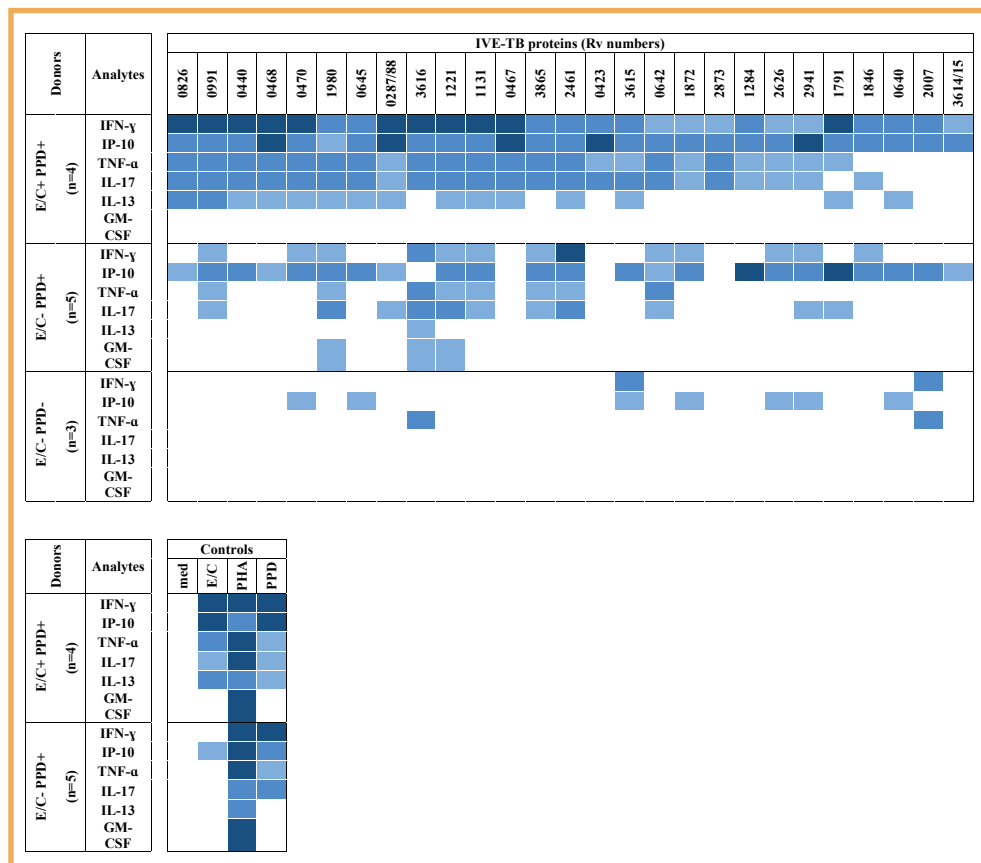


Figure 4. Cytokine production in response to IVE-TB antigens in PBMC of individuals differently exposed to mycobacteria. PBMCs of ESAT/CFP10 (E/C) and PPD *in vitro* positive (+) or negative (-) donors were stimulated with each IVE-TB antigen, E/C, PPD or PHA for six days. The culture supernatants were tested for the presence of IFN- γ , IP-10, TNF- α , IL-17, IL-13, IL-10, and GM-CSF using a seven-plex assay. Results are shown for those IVE-TB antigens which elicited at least two different cytokines in $\geq 50\%$ of the donors.

To compare the level of cytokines induced by each IVE-TB antigen with that produced by E/C, the fold change in the median cytokine levels of stimulated vs. unstimulated samples from the *Mtb*-exposed individuals (double or single responders) was calculated. Notably, distinct cytokine profiles were observed for different antigens (Figure 6; Supplementary Figure 4).

In conclusion, most of the IVE-TB antigens-inducing cytokine responses ($n=27$) were recognised by *Mtb*-exposed individuals by the induction of several cytokines, with responses highly correlated in terms of magnitude and frequency. For cytokines other than IFN- γ , the magnitude of the reactivity to the IVE-TB antigens differed from

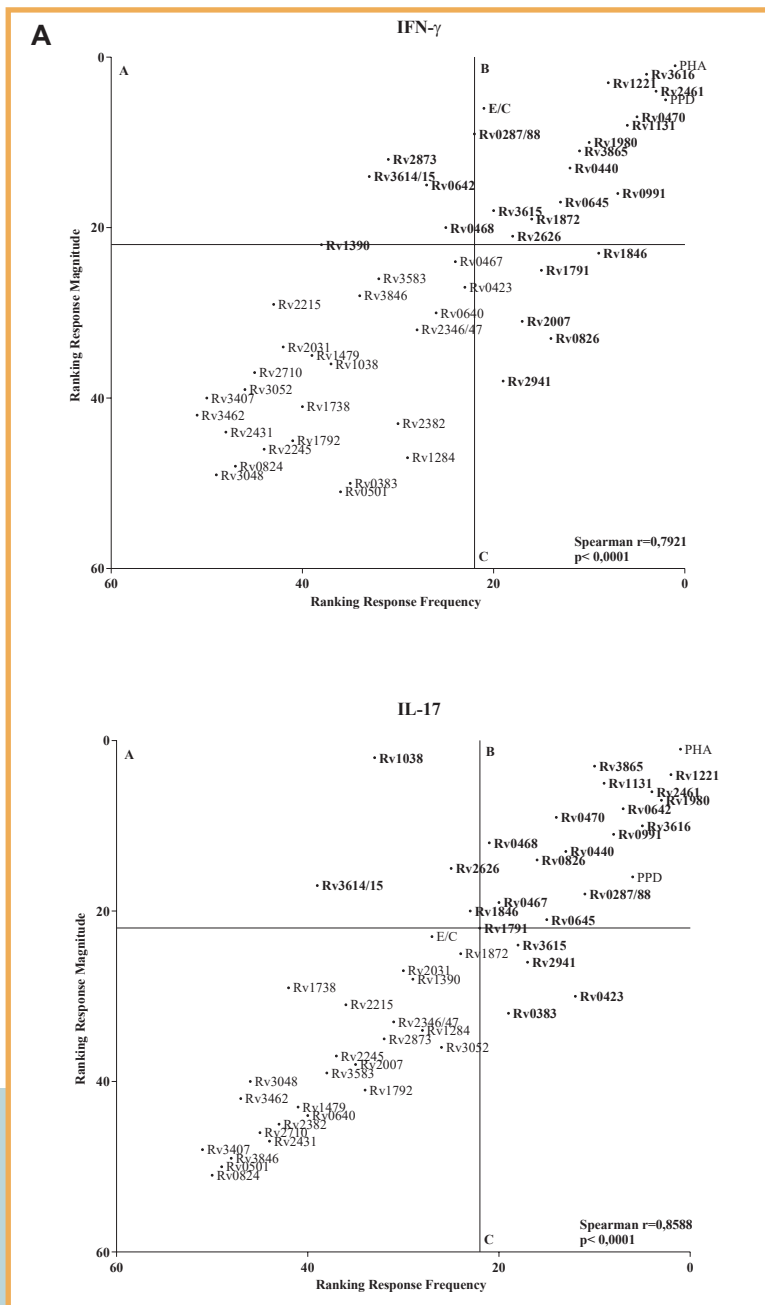


Figure 5. Immunodominance and immunogenicity of IVE-TB antigens based on cytokine production. PBMCs of *Mtb*-responders ($n=$ nine) were stimulated with IVE-TB antigens and tested for the levels of multiple cytokines by multiplex assay. (A) The frequency (x-axis) and the magnitude (y-axis) of responses were ranked to compare the immunodominance and the immunogenicity of each antigen, respectively, per analyte as well as for the responses to the positive controls (PPD and PHA). In quadrant A are the top antigens for immunogenicity,

Continue

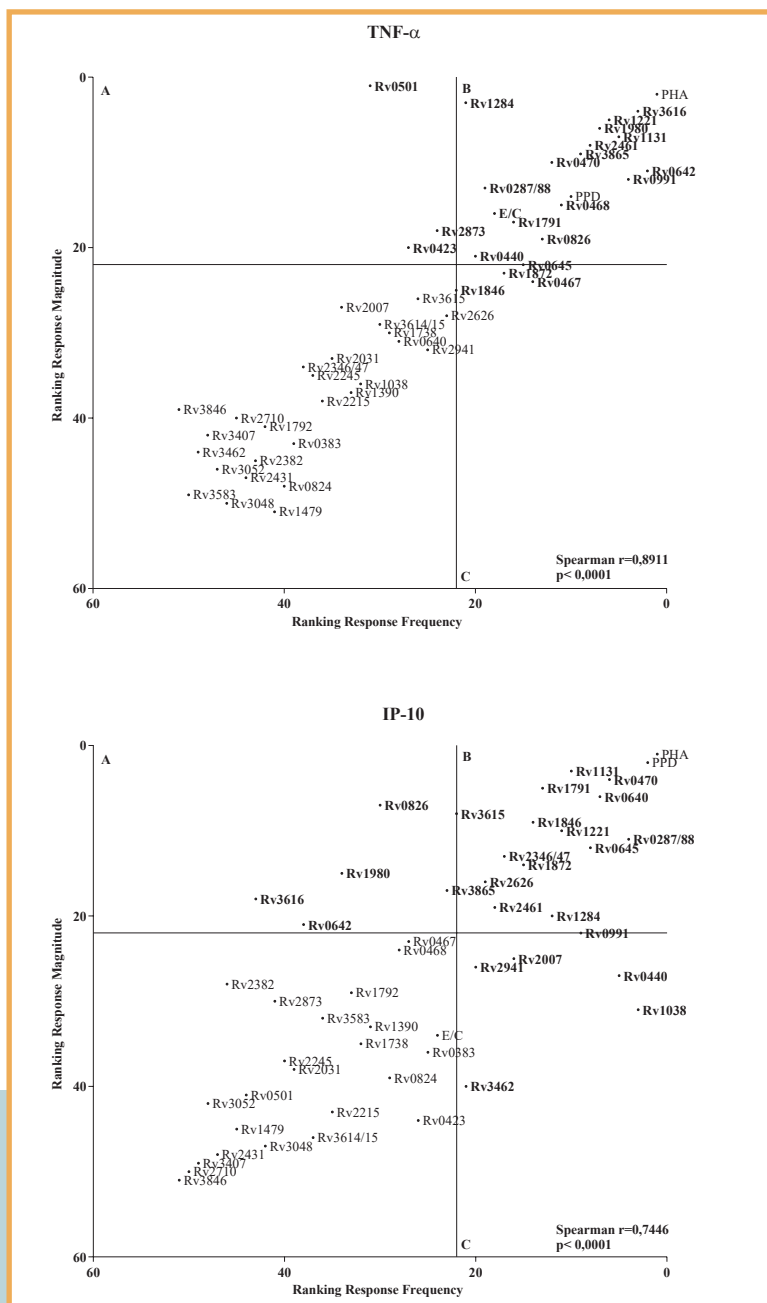


Figure 5 continued

in quadrant C the top antigens for immunodominance, and in quadrant B the top antigens for both parameters. Results were determined by Spearman's rank correlation coefficient. Graphs are shown for IFN- γ , IL-17, TNF- α and IP-10 as examples. (B) Summary of the top immunogenic and/or immunodominant 20 IVE-TB antigens (present in quadrant A, B or C) for all the cytokines analysed.

B

Rv number	Cytokines					
	IFN- γ	IL-13	IL-17	IP-10	TNF- α	GM-CSF
Rv1221						
Rv0287/88						
Rv0470						
Rv0645						
Rv2461						
Rv0991						
Rv1131						
Rv1980						
Rv3616c						
Rv2626						
Rv0440						
Rv3875/74 (ESAT6/CFP10)						
Rv3615						
Rv3865						
Rv1791						
Rv1846						
Rv0468						
Rv0826						
Rv0642						
Rv1872						
Rv1284						
Rv0383						
Rv0640						
Rv2346/47						
Rv0467						
Rv0423						
Rv1038						
Rv1792						
Rv2215						
Rv2382						
Rv2710						
Rv3048						
Rv0642						
Rv3865						
Rv2873						
Rv3614/15						
Rv3407						
Rv0468						
Rv1390						
Rv0826						
Rv1980						
Rv3616c						
Rv0423						
Rv0501						
Rv1038						
Rv1846						
Rv2626						
Rv1131						
Rv3846						
Rv2941						
Rv2007						
Rv1846						
Rv1791						
Rv0826						
Rv0467						
Rv0440						
Rv1038						
Rv3462						
Rv1872						
Rv0383						
Rv0423						
Rv3615						
Rv0640						
Rv0468						
Rv0501						

Antigens ranked in the top 20 immunogenic but not immunodominant IVE-TB proteins analysed (quadrant B)

Antigens ranked in the top 20 immunogenic but not immunodominant IVE-TB proteins analysed (quadrant A)

Antigens ranked in the top 20 immunogenic but not immunodominant IVE-TB proteins analysed (quadrant C)

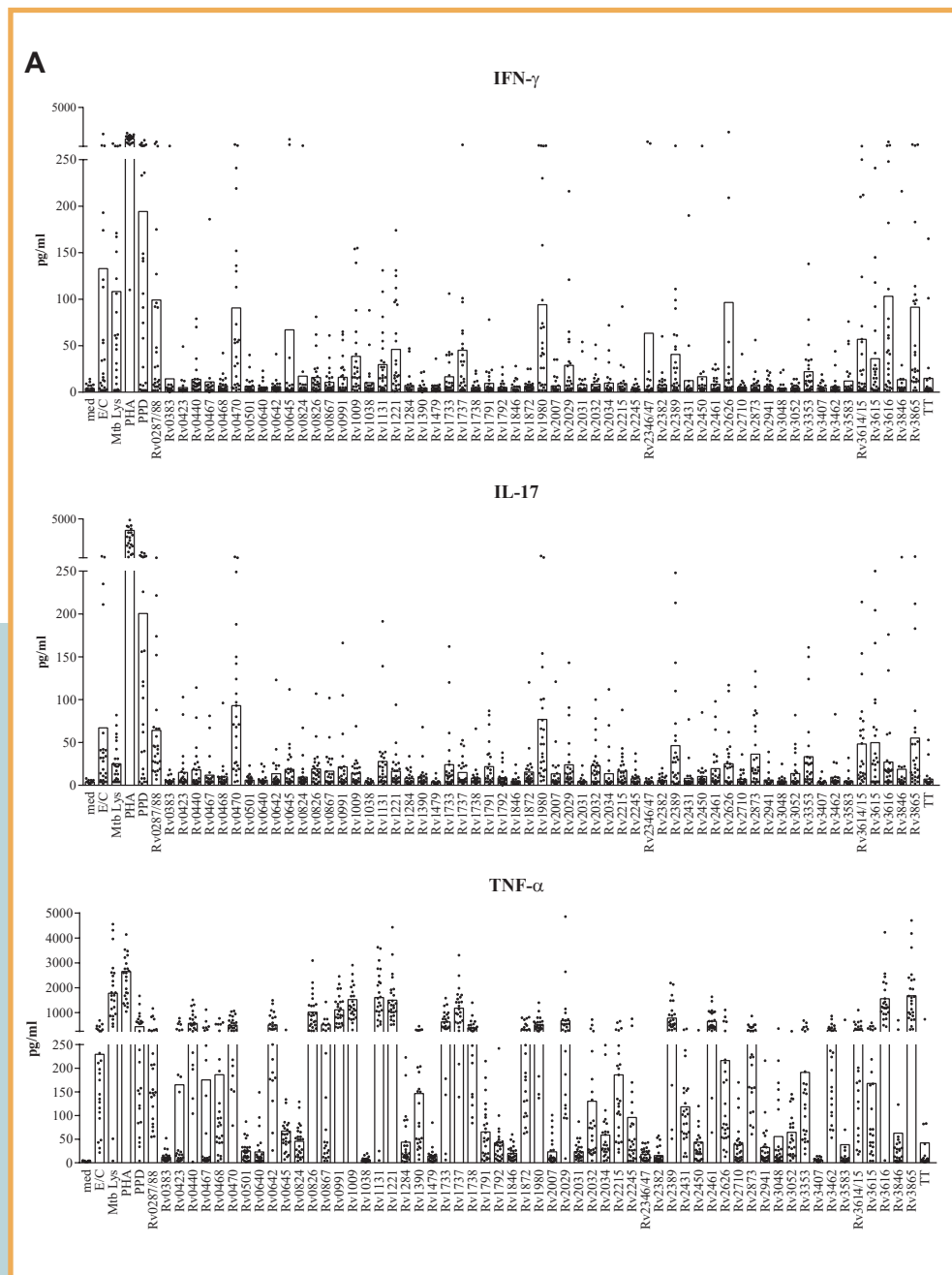
that to E/C. Importantly, many cytokines other than IFN- γ were induced. Especially pro-inflammatory and Th1-related IP-10, TNF, IL-17, and Th2-related IL-13 revealed a much wider response pattern than expected.

Cytokine responses to novel IVE-TB antigens in an independent cohort of latently *Mtb*-infected individuals.

To validate these results in an independent cohort, we evaluated the immunogenicity of the selected IVE-TB proteins in latently *Mtb*-infected (LTBI) donors (n=25). For comparative purposes we also included ten additional *Mtb* antigens identified previously (Rv0867, Rv1009, Rv1733, Rv1737, Rv2029, Rv2032, Rv2034, Rv2389, Rv2450, and Rv3353) (23, 24, 41, 47-54). Diluted whole blood samples were stimulated for six days and the cytokine levels were assessed by a seven-plex assay (data shown only for IFN- γ , IL-17, TNF- α and IP-10 Figure 7A). Significant differences (Dunn's multiple comparisons test) were observed between the unstimulated and the stimulated samples in the levels of all analytes except for IL-13, IL-22, and IL-9 (Figure 7B).

Forty-two out of the 58 antigens significantly increased the production of at least one cytokine, particularly TNF- α . Remarkably, several antigens induced distinct cytokines simultaneously. In this regard, E/C, PHA, PPD and 11 antigens (Rv0287/88, Rv0470, Rv1009, Rv1737, Rv1980, Rv3865, Rv3616, Rv1221, Rv2389, Rv1131, and Rv3614/15) induced substantial and concomitant secretion of IFN- γ , IP-10 and TNF- α , sometimes in combination with IL-17. Notably, several antigens did not induce IFN- γ but nevertheless induced other cytokines. In fact, nine antigens (Rv3615, Rv2029, Rv3353, Rv1733, Rv0826, Rv2215, Rv1791, Rv2873, and Rv2626) simultaneously increased IP-10, TNF- α and IL-17 secretion in the absence of significant IFN- γ . Six antigens (Rv0440, Rv3462, Rv0991, Rv2031, Rv1872, and Rv0645) induced high production of TNF- α in combination with either IL-17 or IP-10 in the absence of significant IFN- γ . No specific association between known functions of the *Mtb* proteins and the pattern of cytokine expression could be distinguished (Supplementary Figure 3).

Collectively, the results demonstrate that this independent cohort of LTBI donors recognised most of the selected IVE-TB antigens as judged by the induction of multiple cytokines, confirming and extending the immunogenicity of the IVE-TB antigens uncovered in this study.



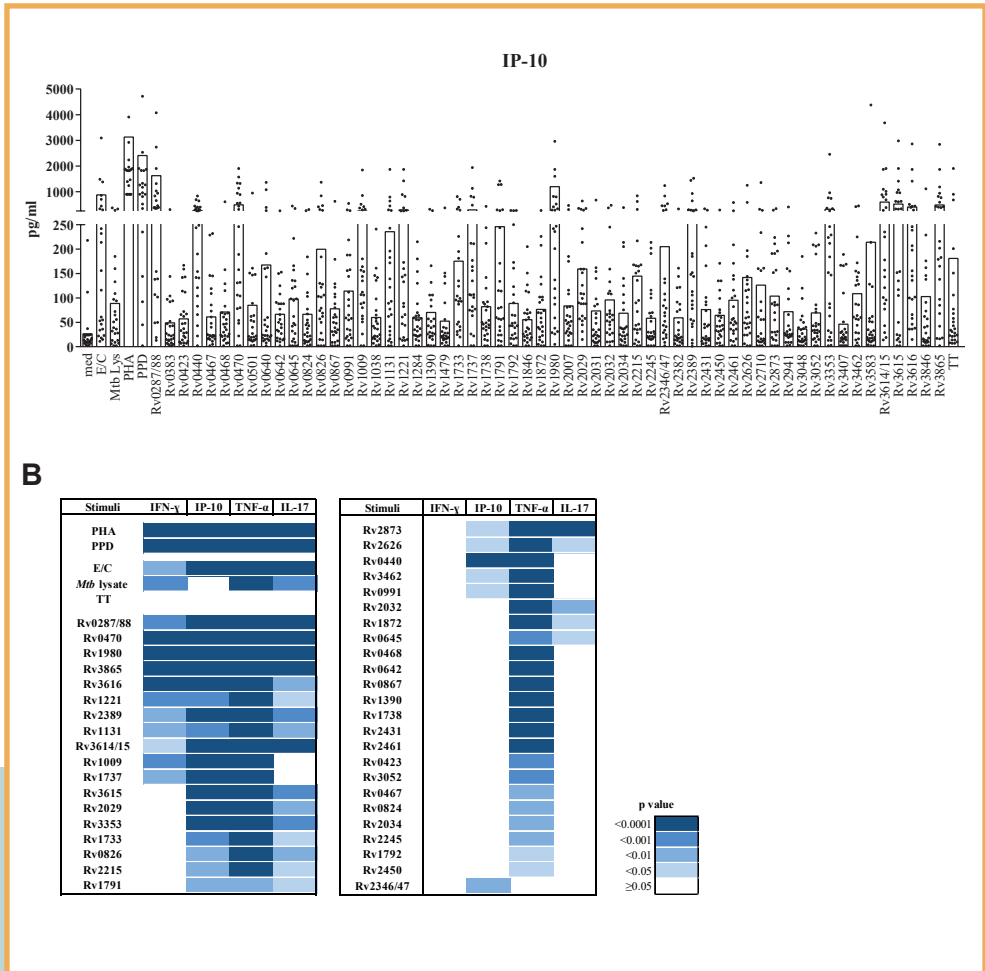


Figure 7. Cytokine response profile to IVE-TB antigens in LTBI. The cytokine levels were measured in diluted whole blood supernatants of an independent cohort of LTBI (n=25) after six days stimulation with either IVE-TB antigens (10 μ g/ml), ESAT6/CFP10 (E/C) (10 μ g/ml), PPD (5 μ g/ml), PHA (2 μ g/ml) or tetanus toxoid (TT) (10 μ g/ml). (A) Bars represent the mean of responses. Results are shown for IFN- γ , IL-17, TNF- α and IP-10 as illustrative examples. (B) Significance differences were evaluated between the cytokine level induced by IVE-TB antigens vs. unstimulated (Dunn's multiple comparisons test).

DISCUSSION

The urgent quest for *Mtb* antigens capable of inducing protective immunity against *Mtb* (16) prompted us to develop a new algorithm to identify novel immunogenic *Mtb* proteins. Several studies have pursued strategies to discover new *Mtb* peptide epitopes and their related antigens using *in silico* predictive tools and functional immunomic approaches (26, 28, 55). However, as far as we are aware, our approach focusing on *in vivo* expressed (IVE-TB) *Mtb* genes (23) is unique, because it concentrates on real-time *in vivo* *Mtb* pulmonary infection-based gene expression data. Our rationale is that effective *Mtb* antigens need to be expressed in the main target organ of *Mtb*, the lung, and should induce significant T cell responses in humans (12, 13, 22).

To follow this track, we have designed a new algorithm to select the 50 most promising *Mtb* IVE-TB genes. We generated a new database by isolating *Mtb* RNA from the lung of highly susceptible (C3HeB/FeJ) as well as genetically resistant (C57BL/6J) mice both at early and late time points after aerosol infection, and analysing the expression of 2,068 *Mtb* genes to allow the selection of the most upregulated IVE-TB genes during early and late phase infection. By combining these data with analysis of high-level conservation in a set of 219 whole-genome sequenced *Mtb* complex strains, and with the presence of predicted HLA class Ia and II peptide binding motifs as well as high homology with other pathogenic mycobacteria, we could identify the most promising IVE-TB candidate antigens. Several of these were well recognized by blood cells from *in vitro* *Mtb* responsive donors and LTBI as measured by T-cell proliferation and multi-cytokine production assays, including antigens that did not induce IFN- γ . The fact that we identified several antigens which are currently in clinical vaccination trials independently underscores the validity of our novel *Mtb* antigen discovery approach as novel tools for TB vaccination and TB biomarker profiling.

The majority of the 50 IVE-TB genes selected in this study were found to be hyperconserved among all *Mtb* lineages as well as in pathogenic or non-tuberculous mycobacteria (NTM) and BCG. Although for other infectious agents, antigen conservation is considered an essential feature to develop vaccines with global immunization coverage (56), this assumption is under debate in the TB field (57). The finding that *Mtb* epitopes recognized by human T-cells are evolutionarily hyper-conserved has been interpreted to suggest that this may benefit the pathogen, and has promoted research into non-conserved, "hyper-variable" *Mtb* antigens and epitopes (58). However, a possible, independent factor influencing this selection of hyper-conserved antigens might be that these *Mtb* sequences encode protein domains essentially required for *Mtb* survival inside the host cell, such that mutations

could impair bacterial fitness and would be selected against (59). Conversely, regions less essential to bacterial fitness might then allow more sequence variation, including epitope variation. *Mtb* indeed uses many other powerful immune evasion mechanisms than epitope variation, such as compromising antigen presentation by bacterial- directed vesicular antigen export (60) and induction of immunoregulatory mechanisms to reduce CD4+ T cell recognition of *Mtb*-infected cells (61). In addition, as others have suggested (62), the observed epitope hyper-conservation might also be the result of previous BCG or NTM exposure, skewing *Mtb* recall antigen responses towards epitopes conserved among multiple mycobacterial species. Therefore, we consider important to include antigens with high homology with BCG/NTM given the opportunity to boost BCG/NTM-induced responses at a later stage in life. In any case, TB vaccination strategies will need to reprogram immune response profiles, including those against conserved antigens, such that protective effector mechanisms are activated without promoting pathology by imbalanced immune activation (59). Therefore, we think that conserved IVE-TB antigens represent important targets for TB vaccination, including their ability to offer global *Mtb* lineage coverage.

The immunogenicity and immunodominance of the selected IVE-TB proteins were demonstrated by the fact that many of them stimulated significant lymphocyte proliferation and multiplex cytokine production in the blood of *Mtb* ESAT6/CFP10 (E/C)- and PPD- responsive *in vitro* individuals. Of note, the magnitude and the frequency of the antigen-induced responses were highly correlated. The use of independent assays and cohorts not only validated the results, but also revealed induction of several cytokines other than IFN- γ , considered relevant for further investigation of T cell responses.

Virtually all *Mtb* antigen discovery approaches thus far have relied on IFN- γ as single or as leading biomarker. Our study significantly broadens this to a wider range of cytokines. The recent failure of a TB vaccine candidate antigen identified mostly based on IFN- γ readouts (9, 11, 12) urges the need for using novel correlates of immunogenicity (63) at an early stage of TB vaccine development. Although some studies have analysed polyfunctional Th1-cells producing IFN- γ , TNF- α , and IL-2 (16, 63, 64), their contribution in TB remains unclear (65), although they seem to be associated primarily with vaccine induced protection in animal studies (66). We have therefore included alternative cytokines which have been previously studied for their role in *Mtb* infection (67-70). Interestingly, some IVE-TB antigens showed enhanced production of cytokines involved not only in Th1 but also in Th17 and Th2 responses. The ability of some IVE-TB antigens to induce Th2 related IL-13 response might be in line with our recent findings on *Mtb* specific HLA-E restricted CD8+ T-cells which had a 'Th2-like' profile, while still being able to actively lyse

Mtb infected cells and inhibit intracellular *Mtb* outgrowth (67). Future studies will address the cellular source(s) of the *Mtb* IVE-TB antigen induced alternative cytokines detected in this study. Of further note, distinct cytokine profiles (in terms of fold-change induction) were observed when selected IVE-TB antigens were compared to E/C. Most of these differences were more prominent for these alternative cytokines than for IFN- γ , underscoring the importance of characterizing the immunogenic potential of novel antigens more broadly than by IFN- γ as a single biomarker. The capability of the selected proteins to induce distinct cytokine responses was further validated in an independent cohort of LTBI donors. Indeed, a large group of IVE-TB antigens induced several cytokines and chemokine, especially TNF- α , IL-17, and IP-10, to an equal or even higher level than known *Mtb* antigens that were included for comparative purposes. As observed previously (28), different 'TubercuList classes' of antigens elicited similar functional immune responses.

From the 48 tested IVE-TB proteins, a total of 29 were able to induce multi-functional cytokine responses in at least one group of *Mtb*-exposed subjects (Figure 8).

Fifteen out of 29 IVE-TB antigens also showed increased proliferation in terms of frequency and magnitude. The differences in cytokine profiles between the two groups of donors (likely exposed to NTM vs. *Mtb*-infected) might further be explained by the different assays used (PBMC vs. diluted whole blood) and donor to donor variability. The observed inter-donor variation in cytokine secretion, which agrees with other studies (71), might also correspond to differences in the phenotype of responding cells, in the level and duration of *Mtb* exposure and in the genotype of the infecting *Mtb* strains (72).

To the best of our knowledge, 17 out of these 29 IVE-TB antigens have not been described previously in terms of immunogenicity. Of note, three out of the 17 novel multifunctional IVE-TB antigens (Rv0645, Rv1131 and Rv2461) were among the seven proteins predicted to have the highest number of HLA class Ia and/or HLA class II peptide binding motifs, confirming the power of the *in silico* prediction tools used in our discovery algorithm. Several of the 29 IVE-TB antigens identified here have been previously reported as being regulated in *in vitro* studies which aimed to replicate *in vivo* stress conditions that *Mtb* encounters inside host cells: the expression of some IVE-TB antigens was described to be affected by nutrient starvation (73) (Rv0287/88, Rv0470c, Rv0640, Rv0645, Rv1221, Rv1284, Rv1980, Rv2873, Rv3614/15, Rv3616, Rv3865), hypoxia (74) (Rv0826, Rv0991c, Rv1221, Rv1284, Rv2007, Rv2626c), exposure to vitamin C (75) (Rv2626c, Rv0467, Rv1221, Rv0991, Rv3615c, Rv3616c) or intra-phagosomal infection in naïve and activated macrophages (76) (Rv0467, Rv0642, Rv0826, Rv1121, Rv1980, Rv2007, Rv2626, Rv2873). This concordance is

consistent with, and validates the contribution of some selected IVE-TB proteins in host-pathogen interactions in early and late phase *Mtb* infection and extends these results indirectly to *in vivo* pulmonary infection. In line with this, many of the IVE-TB antigens have been reported to be essential for *Mtb* (Figure 8) and are highly

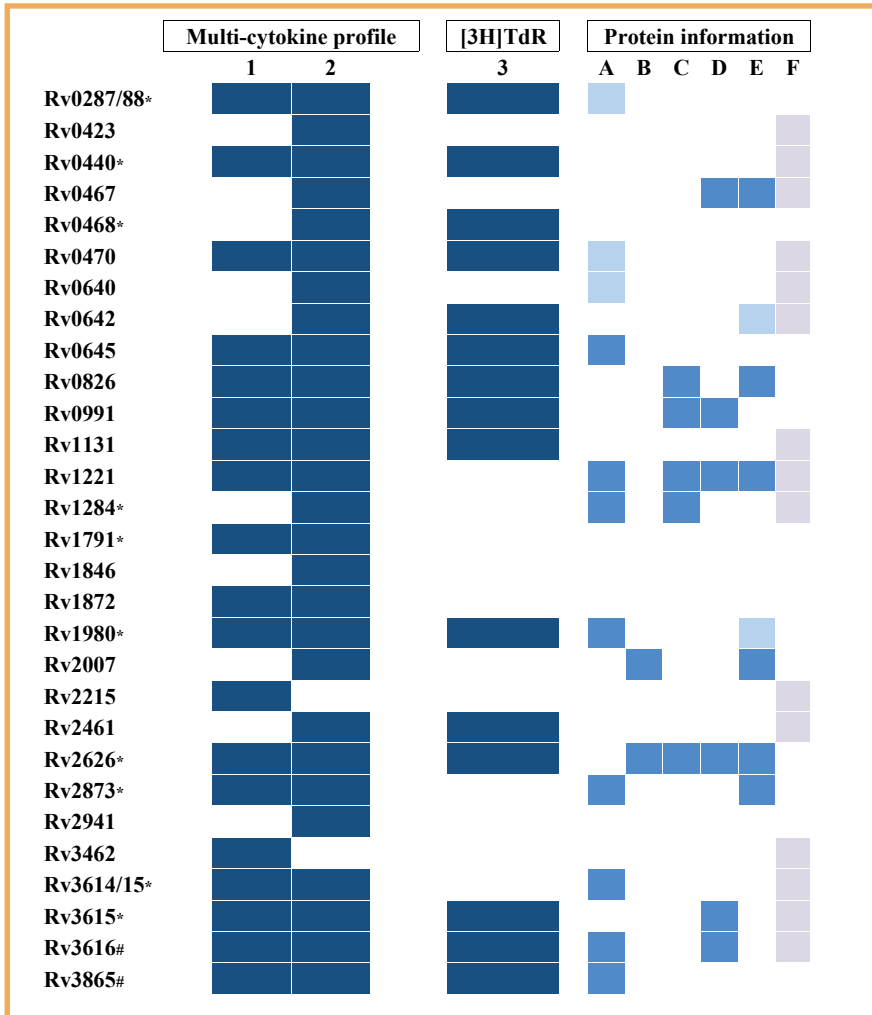


Figure 8. Multifunctional cytokine- and proliferative- responses induced by IVE-TB antigens, combined with literature-based functional assessment. Group of IVE-TB antigens which were able to induce multi-functional cytokine responses in at least one group of *Mtb*-exposed subjects as well as proliferative responses. 1: LTBI group (n = 25); 2: ESAT/CFP10 and PPD *in vitro*+ group (n = 9); 3: E/C and PPD *in vitro*+ group (n = 15); *: known antigen for IFN- γ production (41, 45, 46, 50); #: patent WO 2014063704 A2. A: Nutrient starvation 73; B: DosR 74; C: EHR 74; D: Vitamin C exposure 75; E: intra macrophage expressed genes 76; F: essential (according to TubercuList). ■: induction \geq two cytokines; ■: down-regulated; ■: up-regulated; ■: essential.

homologous to proteins present in pathogenic or nontuberculous mycobacteria (NTM).

We conclude that the combination of our *in vivo* and *in silico* algorithm facilitates the identification of novel IVE-TB antigens, providing new tools for TB vaccination and antigen specific biomarker profiling. The high homology found with other pathogenic mycobacteria, such as *M. leprae* and *M. ulcerans*, might further extend their use as vaccine tools (77, 78). Finally, the generic approach we have presented here can be applied for targeted discovery of antigens to be used in control measures for other infectious disease.

MATERIAL AND METHODS

Mouse strains and murine pulmonary infection for *Mtb* mRNA gene expression.

C3HeB/FeJ (C3H) and C57BL/6J(B6) mice were purchased from The Jackson Laboratory (Bar Harbor, ME, USA) and housed under specific pathogen-free conditions. *Mtb* Erdman strain suspensions (Trudeau Institute, Saranac Lake, NY, USA) were grown to midlog phase, washed and stored at -80°C . Before infection, mycobacteria were thawed, sonicated and diluted in PBS to 10^6 CFU/ml. Mice were aerosol challenged by 25–50 CFU *Mtb* using a Madison chamber (University of Wisconsin, Madison, WI, USA) (79). Four mice per group was sacrificed at five different time points. Studies in mice were performed in agreement with the Guide for the Care and Use of Laboratory Animals and the Animal Welfare Act. The study protocol (No. AN-15276.2016.05) was approved by the Institutional Animal Care and Use Committee of Boston University Medical Center.

Genome-wide *Mtb* mRNA gene expression. Quantification of *Mtb* transcription profile was performed as previously described (19, 23, 80, 81). Total *Mtb* RNA was isolated from infected mouse lung tissue by homogenization in Trizol (Thermo Fisher Scientific, Waltham, MA, USA) and bacillary disruption by bead beating (MP Biomedicals, Solon, OH, USA). Total RNA was purified using RNeasy columns (Qiagen, Valencia, CA, USA). cDNA synthesis was conducted using 50ng total RNA, which was separated in reverse transcriptase (RT)+ and RT- reactions to control for DNA impurity. cDNA was further amplified via controlled multiplex pre-amplification (19). Sequences and design of PCR primer/probe sets are available at <http://genes.stanford.edu/technology.php> and <http://www.tbdb.org/rtpcrData.shtml>. Individual gene transcript quantification was carried out using TaqMan primer/ probe sets (Biosearch Technology, Petaluma, CA, USA). The cycle threshold values generated

were transformed to relative gene copy numbers (RGCNs) based on logarithmic transformation/ linear regression equations devised from calibration curves.

Gene expression analysis. Based on genome-wide, real-time RT-PCR, *Mtb* gene expression patterns of 2,068 genes, mostly representing the first gene of each predicted operon, were analysed from the lungs of infected mice. Those included hypersusceptible C3HeB/FeJ mice (82) and resistant C57BL/6J mice, after two, four, six, nine and twelve wks of *Mtb* challenge. For each time point, the median cycle threshold values of four mice per strain were converted to relative H37 Rv gene copy numbers (RGCNs). For each condition (time point and mouse strain) the RGCNs data were sorted from the highest to the lowest value; genes with RGCNs ranked in the top 15% (n=310) of the ordered list generated 10 datasets (Figure 1A). The threshold of 15% was chosen arbitrarily to limit the number of candidates for further analysis (23). The expression levels observed for the first genes of each predicted operon are considered to extend to the co-regulated genes in the same operons. Microsoft Access 2010 was used to compare and retrieve data shared from all data sets (Supplementary Table 1). Information on the functional classes was obtained from the TubercuList database (<http://tuberculist.epfl.ch/>) (Supplementary Figure 1).

Amino acid conservation. The level of conservation of the 194 candidate genes was determined in 219 whole-genome sequenced *Mtb* complex strains (83), covering all seven known *Mtb* lineages (30). The amino acid (aa) conservation of each gene was expressed as the ratio of number of aminoacid substitutions observed and the number of aa of the protein encoded by the examined gene. All the genes with a ratio of $\geq 98\%$, an arbitrarily chosen cut-off value, were considered hyper-conserved (Supplementary Table 2 available online at: https://static-content.springer.com/esm/art%3A10.1038%2Fsrp37793/MediaObjects/41598_2016_BFsrep37793_MOESM1_ESM.pdf).

Structures of the proteins. For each gene, aa length and predicted transmembrane motifs were checked in the TubercuList database (<http://tuberculist.epfl.ch/>) and Hidden Markov Models (<http://www.cbs.dtu.dk/services/TMHMM/TMHMM2.0b.guide.php>) (84). Encoded proteins with a length > 600 aa or including predicted transmembrane regions, with a probability above one or with multiple transmembrane regions, were excluded.

Presence of peptide binding motifs for HLA class Ia and class II. The following methods were used with FASTA format input files: NetMHCcons 1.0 ([cbs.dtu.dk/services/NetMHCcons](http://www.cbs.dtu.dk/services/NetMHCcons)) was employed to identify 9-mer peptides containing a peptide binding motif for 12 HLA class Ia supertype representatives (HLA-A1, -A2, -A3, -A24,

-A26, -B7, -B8, -B27, -B39, -B44, -B58 and -B62) (31) and NetMHCIIpan 3.0 (cbs.dtu.dk/services/NetMHCIIpan) (32) was employed to identify 15-mer peptides containing an HLA- peptide binding motif for 29 common HLA-DR, -DQ and -DP molecules, including 27 alleles: 15 HLA-DR, 6 HLA-DQ and 6 HLA-DP (DRB1*01:01; DRB1*03:01; DRB1*04:01; DRB1*07:01; DRB1*04:05; DRB1*08:02; DRB1*09:01; DRB1*11:01; DRB1*12:01; DRB1*13:02; DRB1*15:01; DRB3*01:01, DRB3*02:02; DRB4*01:01; DRB5*01:01; HLA DQA1*05:01-DQB1*02:01; HLA-DQA1*05:01-DQB1*03:01; HLA-DQA1*03:01-DQB1*03:02; HLA-DQA1*04:01-DQB1*04:02; HLA-DQA1*01:01-DQB1*05:01; HLA-DQA1*01:02-DQB1*06:02; HLA-DPA1*02:01-DPB1*01:01; HLA-DPA1*01:03-DPB1*02:01; HLA-DPA1*01:03-DPB1*04:01; HLA-DPA1*03:01-DPB1*04:02; HLA-DPA1*02:01-DPB1*05:01; HLA-DPA1*01:03-DPB1*14:01). These alleles represent approximately 50–75% of all allelic variants at each of the class II loci considered in the study of Greenbaum (34), whereas DRB1_0803 and DRB1_1402 were extrapolated from a study on the functional similarities between the MHC-II molecules (85). To quantitatively analyse the distribution of HLA alleles, we counted and summed the number of HLA class Ia alleles (including 12 HLA class Ia supertypes) (33) and HLA class II alleles (including 17 HLA class II frequent alleles) (34) covered by predicted peptide binding motifs for each protein of interest. If the sum was greater than 20, the protein was considered to have wide HLA coverage (Supplementary Table 4). To avoid bias due to the protein size, the ratio of the number of predicted epitopes (NB) to the length of the proteins (len) was calculated (NB:len). The ranking of proteins with the highest number of predicted binding motifs was based on this ratio (Supplementary Table 4 available online at: https://static-content.springer.com/esm/art%3A10.1038%2Fsrep37793/MediaObjects/41598_2016_BFsrep37793_MOESM1_ESM.pdf).

Protein sequence homology. The homology of selected proteins was studied using BLASTp program (<http://blast.ncbi.nlm.nih.gov/>; January 2015). The query included BCG (taxid: 33892), *M. leprae* (taxid: 1769), *M. avium* (taxid:1764), *M. ulcerans* (taxid:1809) and *M. kansasii* (taxid:1768) (Supplementary Table 3 available online at: https://static-content.springer.com/esm/art%3A10.1038%2Fsrep37793/MediaObjects/41598_2016_BFsrep37793_MOESM1_ESM.pdf).

Recombinant proteins. As described previously (86), *Mtb* genes were amplified by PCR from genomic H37Rv DNA and cloned by Gateway technology (Invitrogen, Carlsbad, CA, USA) in a bacterial expression vector containing a histidine (His) tag at the N-terminus. Vectors were overexpressed in *Escherichia coli* (*E. coli*) BL21 (DE3) and purified. The size and purity of the recombinant proteins were analysed by gel electrophoresis and western blotting with an anti-His Ab (Invitrogen) and an anti-*E. coli* polyclonal Ab (gift of Statens Serum Institute, Copenhagen, Denmark). Rv0287-

Rv0288, Rv2346c-Rv2347, and Rv3614-Rv3615 were prepared as fusion proteins (29) to mimic the pairwise dependent secretion pathway followed by T7S systems (87). At this point, two proteins (Rv1197 and Rv1831) were excluded due to problems linked to their production. Forty-eight recombinant proteins were produced and tested to exclude protein-nonspecific T-cell stimulation and cellular toxicity (50).

Study subjects included. To assess T-cell proliferation after stimulation with the selected IVE-TB proteins, we used PBMC from 19 healthy Dutch donors. From these stimulated samples, the supernatant of 12 donors was tested with a multiplex cytokine assay (7-plex). Twenty-five latently *Mtb*-infected (LTBI) individuals, defined by a Mantoux tuberculin skin test (TST) ≥ 15 mm and/or a QuantiFERON-TB Gold In-Tube test (QFT-GIT) (Cellestis, Carnegie, VIC, Australia) ≥ 0.3 IU/ml, were recruited via the Dutch health service and diluted whole blood assay and multiplex cytokine array were performed. The study protocol (P07.048) was approved by the Institutional Board of the Leiden University Medical Center, The Netherlands. Informed written consent was required to participate in the study and was obtained before to collect blood samples.

Lymphocyte stimulation test and thymidine incorporation assay. PBMC (1.5×10^5) were cultured in AIM-V medium (Invitrogen, Breda, The Netherlands) in triplicate in 96-well round-bottom plates (Nunc, Roskilde, Denmark) and incubated at 37°C and 5% CO₂. The IVE-TB proteins were tested at a final concentration of 10 μ g/ml. As controls, 5- μ g/ml PPD (Statens Serum Institute, Copenhagen, Denmark) and 2- μ g/ml PHA (Remel, Oxoid, Haarlem, The Netherlands) were included. After six days, the supernatants were used for cytokine determination as previously described (24). Tritium thymidine was added for the last 16 hours of culture after which the cells were harvested and counted on a Microbetaplate counter (Wallac, Turku, Finland). The Stimulation Index (SI) was calculated as the ratio of the median counts per minute (cpm) of the stimulated samples to the median cpm without stimulation. SI values \geq three were considered positive for proliferation.

Multiplex cytokine array performed with PBMC supernatants. The concentrations of seven analytes (IL-13, IL-10, IL-17A, IFN- γ , IFN- γ -induced protein 10 [IP-10 (CXCL10)], GM-CSF and TNF- α) in the supernatants of stimulated PBMCs were assessed. Data were acquired using the Bio-Plex suspension array system powered by Luminex xMap multiplex technology (Bio-Rad Laboratories, Veenendaal, The Netherlands) and analysed using Bio-Plex Manager software 6.0 (Bio-Rad Laboratories), as previously described (88). For all cytokines the background value of unstimulated samples was below 25 pg/ml and therefore we considered values >50 pg/ml as relevant. Only for IFN- γ , the background ranged between 23 and

83 pg/ml and therefore the cut-off was set at 100 pg/ml (in agreement with our previous studies). For IP-10, due to the large spread of the values measured in the unstimulated samples (37-8213 pg/ml), we subtracted the backgrounds, and we considered positive the responses over or equal than 250 pg/ml (three times the lowest detection limit of the IP-10 standard curve).

Diluted whole blood assay. Within 3 hours of collection, heparinized venous blood was diluted 1:10 in AIM-V medium (Invitrogen, Breda, The Netherlands). Samples were incubated (450 μ l/well) in 48-well plates at 37°C at 5% CO₂, 90% relative humidity, with 50 μ l antigen solution (final concentration of 10 μ g/ml). After 24 hours, 200 μ l of the supernatants were collected from each well and frozen in aliquots at -20°C until further analysis.

Multiple cytokine array and analysis of diluted whole blood supernatant. A human R&D™ premixed multi-analyte kit was used to measure IL-13, IL-22, IL-17A, IFN- γ , IP-10, IL-9 and TNF- α in diluted whole blood culture supernatants according to manufacturer's instructions. Values outside the upper or lower limits of quantification were set as the values of the analyte detection limits.

Statistical analysis. Statistical analysis was performed using Graph Pad Prism (version 6.0). A Spearman nonparametric correlation was calculated to compare the immunodominance and immunogenicity of the IVE-TB antigens in different immunoassays. The ranking response frequency was calculated as follows: for each antigen the number of positive hits observed in the group of donors analysed was counted and the sum of positive responses for each antigen was obtained. These sums were used to rank the antigens according to their ability to induce a positive response. Similarly, the ranking response magnitude was based on the cumulative response measured among donors to each antigen (55). The Mann-Whitney test was used to compare the difference between groups of donors based on the number of antigens recognised and the magnitude of response induced by stimulation with the antigens. Dunn's multiple comparisons test was performed to analyse the difference between each antigen and the unstimulated samples for all cytokines measured in the LTBI samples. A p-value less than 0.05 was considered significant.

ACKNOWLEDGEMENTS

We acknowledge funding by EC HORIZON2020 TBVAC2020 (Grant Agreement No. 643381); EC ITN FP7 VACTRAIN project (the text represents the authors' views and does not necessarily represent a position of the Commission who will not be liable

for the use made of such information), The Netherlands Organization for Scientific Research (NWO-TOP Grant Agreement No. 91214038); European Research Council (ERC TB-ACCELERATE Grant Agreement NO. 638553). The funders had no role in study design, data collection and analysis, decision to publish, or preparation of the manuscript.

AUTHOR CONTRIBUTIONS

THMO, AG, MC and KEvM participated in the design of the study. KF, IC, IK, OL, CP, GK and FO provided study materials, samples, animals, and computing resources. MC KEvM, KLMCF, GD, GKS and SJFvdE performed the experiments. MC, KM, SC, IC, AG and THMO participated in the data analysis. MC, AG and THMO participated in drafting the paper. THMO supervised the work. All authors reviewed the manuscript.

CONFLICT OF INTEREST STATEMENT

The authors declare no competing financial interests.

REFERENCES

1. WHO. WHO report on the proposed post-2015 TB Strategy and targets. 2013.
2. Uplekar, M. et al. WHO's new end TB strategy. *Lancet* 385, 1799-1801 (2015).
3. Fonseca, J.D., Knight, G.M., & McHugh, T.D. The complex evolution of antibiotic resistance in *Mycobacterium tuberculosis*. *Int. J. Infect. Dis.* 32, 94-100 (2015).
5. WHO. Global tuberculosis report 2015. Geneva: World Health Organization. 2015.
6. Clifford, V., He, Y., Zufferey, C., Connell, T., & Curtis, N. Interferon gamma release assays for monitoring the response to treatment for tuberculosis: A systematic review. *Tuberculosis*. (Edinb.) 95, 639-650 (2015).
7. Fogel, N. Tuberculosis: a disease without boundaries. *Tuberculosis*. (Edinb.) 95, 527-531 (2015).
8. da, C.C., Walker, B., & Bonavia, A. Tuberculosis vaccines—state of the art, and novel approaches to vaccine development. *Int. J. Infect. Dis.* 32, 5-12 (2015).
9. Orme, I.M. Tuberculosis vaccine types and timings. *Clin. Vaccine Immunol.* 22, 249-257 (2015).
10. Frick M. The Tuberculosis Vaccines Pipeline: A New Path to the Same Destination? <http://www.pipelinereport.org/2015/tb-vaccines>. 2015.
11. Geluk, A., van Meijgaarden, K.E., Joosten, S.A., Commandeur, S., & Ottenhoff, T.H. Innovative Strategies to Identify *M. tuberculosis* Antigens and Epitopes Using Genome-Wide Analyses. *Front Immunol.* 5, 256 (2014).
12. Andersen, P. & Kaufmann, S.H. Novel vaccination strategies against tuberculosis. *Cold Spring Harb. Perspect. Med.* 4, (2014).
13. Moliva, J.I., Turner, J., & Torrelles, J.B. Prospects in *Mycobacterium bovis* Bacille Calmette et Guerin (BCG) vaccine diversity and delivery: why does BCG fail to protect against tuberculosis? *Vaccine* 33, 5035-5041 (2015).
14. Tameris, M.D. et al. Safety and efficacy of MVA85A, a new tuberculosis vaccine, in infants previously vaccinated with BCG: a randomised, placebo-controlled phase 2b trial. *Lancet* 381, 1021-1028 (2013).
15. O'Shea, M.K. & McShane, H. A review of clinical models for the evaluation of human TB vaccines. *Hum. Vaccin. Immunother.* 1-11 (2016).
16. Leung-Theung-Long, S et al. A Novel MVA-Based Multiphasic Vaccine for Prevention or Treatment of Tuberculosis Induces Broad and Multifunctional Cell-Mediated Immunity in Mice and Primates. *PLoS. One.* 10, e0143552 (2015).
17. Baldwin, S.L. et al. Protection and long-lived immunity induced by the ID93/GLA-SE vaccine candidate against a clinical *Mycobacterium tuberculosis* isolate. *Clin. Vaccine Immunol.* (2015).
18. Bertholet, S. et al. Identification of human T cell antigens for the development of vaccines against *Mycobacterium tuberculosis*. *J. Immunol.* 181, 7948-7957 (2008).
19. Aagaard, C. et al. A multistage tuberculosis vaccine that confers efficient protection before and after exposure. *Nat. Med.* 17, 189-194 (2011).
20. Luabeya, A.K. et al. First-in-human trial of the post-exposure tuberculosis vaccine H56:IC31 in *Mycobacterium tuberculosis* infected and non-infected healthy adults. *Vaccine* 33, 4130-4140 (2015).
21. Orme, I.M., Robinson, R.T., & Cooper, A.M. The balance between protective and pathogenic immune responses in the TB-infected lung. *Nat. Immunol.* 16, 57-63 (2015).
22. Behar, S.M., Carpenter, S.M., Booty, M.G., Barber, D.L., & Jayaraman, P. Orchestration of pulmonary T cell immunity during *Mycobacterium tuberculosis* infection: immunity interruptus. *Semin. Immunol.* 26, 559-577 (2014).

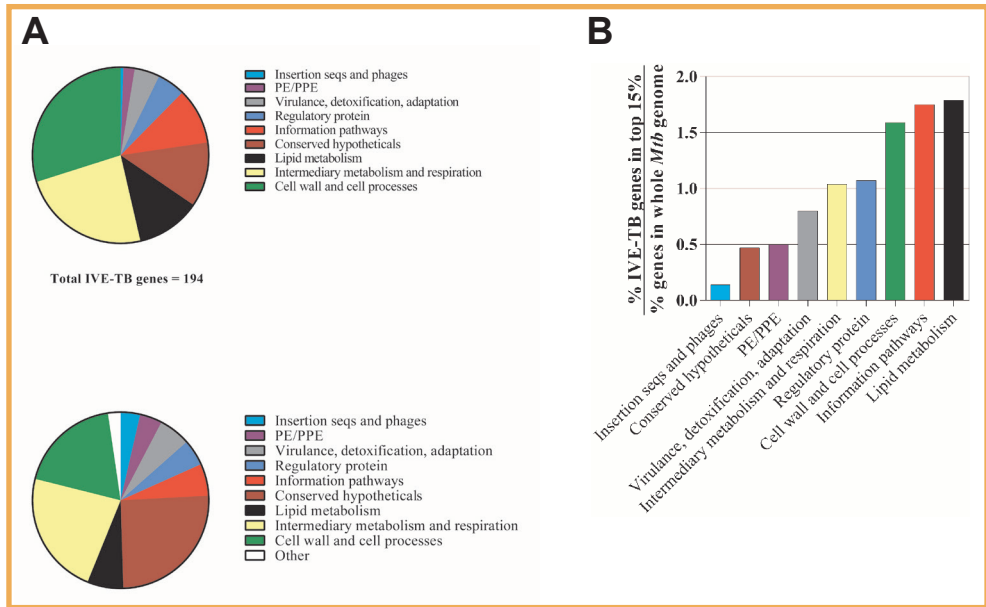
23. Commandeur,S. et al. An unbiased genome-wide *Mycobacterium tuberculosis* gene expression approach to discover antigens targeted by human T cells expressed during pulmonary infection. *J. Immunol.* 190, 1659-1671 (2013).
24. Commandeur,S. et al. Clonal analysis of the T-cell response to *in vivo* expressed *Mycobacterium tuberculosis* protein Rv2034, using a CD154 expression based T-cell cloning method. *PLoS. One.* 9, e99203 (2014).
25. Commandeur,S. et al. The *in vivo* expressed *Mycobacterium tuberculosis* (IVE-TB) antigen Rv2034 induces CD4(+) T-cells that protect against pulmonary infection in HLA-DR transgenic mice and guinea pigs. *Vaccine* 32, 3580-3588 (2014).
26. Lewinsohn,D.M. et al. Human CD8 T Cell Antigens/Epitopes Identified by a Proteomic Peptide Library. *PLoS. One.* 8, e67016 (2013).
27. Joosten, S.A. et al. *Mycobacterium tuberculosis* peptides presented by HLA-E molecules are targets for human CD8 T-cells with cytotoxic as well as regulatory activity. *PLoS. Pathog.* 6, e1000782 (2010).
28. Lindestam Arlehamn, C.S. et al. Memory T cells in latent *Mycobacterium tuberculosis* infection are directed against three antigenic islands and largely contained in a CXCR3+CCR6+ Th1 subset. *PLoS. Pathog.* 9, e1003130 (2013).
29. Knudsen, N.P. et al. Tuberculosis vaccine with high predicted population coverage and compatibility with modern diagnostics. *Proc. Natl. Acad. Sci. U. S. A* 111, 1096-1101 (2014).
30. Comas,I. et al. Out-of-Africa migration and Neolithic coexpansion of *Mycobacterium tuberculosis* with modern humans. *Nat. Genet.* 45, 1176-1182 (2013).
31. Karosiene,E., Lundegaard,C., Lund,O., & Nielsen,M. NetMHCcons: a consensus method for the major histocompatibility complex class I predictions. *Immunogenetics* 64, 177-186 (2012).
32. Karosiene,E. et al. NetMHCIpan-3.0, a common pan-specific MHC class II prediction method including all three human MHC class II isotypes, HLA-DR, HLA-DP and HLA-DQ. *Immunogenetics* 65, 711-724 (2013).
33. Sidney,J., Peters,B., Frahm,N., Brander,C., & Sette,A. HLA class I supertypes: a revised and updated classification. *BMC. Immunol.* 9, 1 (2008).
34. Greenbaum,J. et al. Functional classification of class II human leukocyte antigen (HLA) molecules reveals seven different supertypes and a surprising degree of repertoire sharing across supertypes. *Immunogenetics* 63, 325-335 (2011).
35. Duthie, M.S. et al. Protection against *Mycobacterium leprae* infection by the ID83/GLA-SE and ID93/GLA-SE vaccines developed for tuberculosis. *Infect. Immun.* 82, 3979-3985 (2014).
36. Gillis,T.P., Tullius,M.V., & Horwitz,M.A. rBCG30-induced immunity and cross-protection against *Mycobacterium leprae* challenge are enhanced by boosting with the *Mycobacterium tuberculosis* 30-kilodalton antigen 85B. *Infect. Immun.* 82, 3900-3909 (2014).
37. Batista-Silva,L.R. et al. *Mycobacterium leprae*-induced Insulin-like Growth Factor I attenuates antimicrobial mechanisms, promoting bacterial survival in macrophages. *Sci. Rep.* 6, 27632 (2016).
38. Reither,K. et al. Safety and immunogenicity of H1/IC31(R), an adjuvanted TB subunit vaccine, in HIV-infected adults with CD4+ lymphocyte counts greater than 350 cells/mm³: a phase II, multi-centre, double-blind, randomized, placebo-controlled trial. *PLoS. One.* 9, e114602 (2014).
39. Reece,S.T. et al. Improved long-term protection against *Mycobacterium tuberculosis* Beijing/W in mice after intra-dermal inoculation of recombinant BCG expressing latency associated antigens. *Vaccine* 29, 8740-8744 (2011).
40. Hoang,T. et al. ESAT-6 (EsxA) and TB10.4 (EsxH) based vaccines for pre- and post-exposure tuberculosis vaccination. *PLoS. One.* 8, e80579 (2013).
41. Leyten, E.M. et al. Human T-cell responses to 25 novel antigens encoded by genes of the dormancy regulon of *Mycobacterium tuberculosis*. *Microbes. Infect.* 8, 2052-2060 (2006).

42. Commandeur,S. et al. Identification of human T-cell responses to *Mycobacterium tuberculosis* resuscitation-promoting factors in long-term latently infected individuals. *Clin. Vaccine Immunol.* 18, 676-683 (2011).
43. Hoff, S.T. et al. Sensitivity of C-Tb: a novel RD-1-specific skin test for the diagnosis of tuberculosis infection. *Eur. Respir. J.* (2015).
44. Young,S. et al. Manipulation of immune responses to *Mycobacterium bovis* by vaccination with IL-2- and IL-18-secreting recombinant bacillus Calmette Guerin. *Immunol. Cell Biol.* 80, 209-215 (2002).
45. Woodworth, J.S. et al. Protective CD4 T cells targeting cryptic epitopes of *Mycobacterium tuberculosis* resist infection-driven terminal differentiation. *J. Immunol.* 192, 3247-3258 (2014).
46. Anthony, D.D. et al. Dissecting the T Cell Response: Proliferation Assays vs. Cytokine Signatures by ELISPOT. *Cells* 1, 127-140 (2012).
47. Essone,P.N. et al. Host cytokine responses induced after overnight stimulation with novel *M. tuberculosis* infection phase-dependent antigens show promise as diagnostic candidates for TB disease. *PLoS. One.* 9, e102584 (2014).
48. Flores Valdez,M.A. & Schoolnik,G.K. DosR-regulon genes induction in *Mycobacterium bovis* BCG under aerobic conditions. *Tuberculosis. (Edinb.)* 90, 197-200 (2010).
49. Kassa,D. et al. Analysis of immune responses against a wide range of *Mycobacterium tuberculosis* antigens in patients with active pulmonary tuberculosis. *Clin. Vaccine Immunol.* 19, 1907-1915 (2012).
50. Coppola,M. et al. Synthetic Long Peptide Derived from *Mycobacterium tuberculosis* Latency Antigen Rv1733c Protects against Tuberculosis. *Clin. Vaccine Immunol.* 22, 1060-1069 (2015).
51. Sutherland, J.S. et al. Analysis of host responses to *Mycobacterium tuberculosis* antigens in a multi-site study of subjects with different TB and HIV infection states in sub-Saharan Africa. *PLoS. One.* 8, e74080 (2013).
52. Romano,M. et al. Potential of *Mycobacterium tuberculosis* resuscitation-promoting factors as antigens in novel tuberculosis sub-unit vaccines. *Microbes. Infect.* 14, 86-95 (2012).
53. Serra-Vidal,M.M. et al. Immunogenicity of 60 novel latency-related antigens of *Mycobacterium tuberculosis*. *Front Microbiol.* 5, 517 (2014).
54. Choi, H.G. et al. *Mycobacterium tuberculosis* RpfE promotes simultaneous Th1- and Th17-type T-cell immunity via TLR4-dependent maturation of dendritic cells. *Eur. J. Immunol.* 45, 1957-1971 (2015).
55. Carpenter,C. et al. A side-by-side comparison of T cell reactivity to fifty-nine *Mycobacterium tuberculosis* antigens in diverse populations from five continents. *Tuberculosis. (Edinb.)* 95, 713-721 (2015).
56. Doolan,D.L., Apte,S.H., & Proietti,C. Genome-based vaccine design: the promise for malaria and other infectious diseases. *Int. J. Parasitol.* 44, 901-913 (2014).
57. Woodworth,J.S. & Andersen,P. Reprogramming the T Cell Response to Tuberculosis. *Trends Immunol.* 37, 81-83 (2016).
58. Coscolla,M. et al. *M. tuberculosis* T Cell Epitope Analysis Reveals Paucity of Antigenic Variation and Identifies Rare Variable TB Antigens. *Cell Host. Microbe* (2015).
59. Woodworth,J.S. & Andersen,P. Reprogramming the T Cell Response to Tuberculosis. *Trends Immunol.* (2016).
60. Srivastava,S., Grace,P.S., & Ernst,J.D. Antigen Export Reduces Antigen Presentation and Limits T Cell Control of *M. tuberculosis*. *Cell Host. Microbe* 19, 44-54 (2016).
61. Ottenhoff,T.H. New pathways of protective and pathological host defense to mycobacteria. *Trends Microbiol.* 20, 419-428 (2012).
62. Lindestam Arlehamn, C.S. et al. Immunological consequences of intragenus conservation of *Mycobacterium tuberculosis* T-cell epitopes. *Proc. Natl. Acad. Sci. U. S. A* 112, E147-E155 (2015).

63. Bhatt,K., Verma,S., Ellner,J.J., & Salgame,P. Quest for correlates of protection against tuberculosis. *Clin. Vaccine Immunol.* 22, 258-266 (2015).
64. Commandeur,S. et al. Double- and monofunctional CD4(+) and CD8(+) T-cell responses to *Mycobacterium tuberculosis* DosR antigens and peptides in long-term latently infected individuals. *Eur. J. Immunol.* 41, 2925-2936 (2011).
65. Caccamo,N. et al. Multifunctional CD4(+) T cells correlate with active *Mycobacterium tuberculosis* infection. *Eur. J. Immunol.* 40, 2211-2220 (2010).
66. Geluk,A. et al. A multistage-polyepitope vaccine protects against *Mycobacterium tuberculosis* infection in HLA-DR3 transgenic mice. *Vaccine* 30, 7513-7521 (2012).
67. van Meijgaarden,K.E. et al. Human CD8+ T-cells recognizing peptides from *Mycobacterium tuberculosis* (Mtb) presented by HLA-E have an unorthodox Th2-like, multifunctional, Mtb inhibitory phenotype and represent a novel human T-cell subset. *PLoS. Pathog.* 11, e1004671 (2015).
68. Jasenosky,L.D., Scriba,T.J., Hanekom,W.A., & Goldfeld,A.E. T cells and adaptive immunity to *Mycobacterium tuberculosis* in humans. *Immunol. Rev.* 264, 74-87 (2015).
69. Parkash,O., Agrawal,S., & Madhan,K.M. T regulatory cells: Achilles' heel of *Mycobacterium tuberculosis* infection? *Immunol. Res.* 62, 386-398 (2015).
70. Toulza,F., Tsang,L., Ottenhoff,T.H., Brown,M., & Dockrell,H.M. *Mycobacterium tuberculosis*-specific CD4(+) T-cell response is increased, and Treg cells decreased, in anthelmintic-treated patients with latent TB. *Eur. J. Immunol.* 46, 752-761 (2016).
71. Fan,L., Xiao,H.P., Hu,Z.Y., & Ernst,J.D. Variation of *Mycobacterium tuberculosis* antigen-specific IFN-gamma and IL-17 responses in healthy tuberculin skin test (TST)-positive human subjects. *PLoS. One.* 7, e42716 (2012).
72. Gagneux,S. et al. Variable host-pathogen compatibility in *Mycobacterium tuberculosis*. *Proc. Natl. Acad. Sci. U. S. A* 103, 2869-2873 (2006).
73. Betts,J.C., Lukey,P.T., Robb,L.C., McAdam,R.A., & Duncan,K. Evaluation of a nutrient starvation model of *Mycobacterium tuberculosis* persistence by gene and protein expression profiling. *Mol. Microbiol.* 43, 717-731 (2002).
74. Rustad,T.R., Harrell,M.I., Liao,R., & Sherman,D.R. The enduring hypoxic response of *Mycobacterium tuberculosis*. *PLoS. One.* 3, e1502 (2008).
75. Sikri,K. et al. The pleiotropic transcriptional response of *Mycobacterium tuberculosis* to vitamin C is robust and overlaps with the bacterial response to multiple intracellular stresses. *Microbiology* 161, 739-753 (2015).
76. Schnappinger,D. et al. Transcriptional Adaptation of *Mycobacterium tuberculosis* within Macrophages: Insights into the Phagosomal Environment. *J. Exp. Med.* 198, 693-704 (2003).
77. Richardus,J.H., Saunderson,P., & Smith,C. Will new tuberculosis vaccines provide protection against leprosy? *Int. J. Tuberc. Lung Dis.* 15, 143 (2011).
78. Phillips,R.O. et al. Effectiveness of routine BCG vaccination on buruli ulcer disease: a case-control study in the Democratic Republic of Congo, Ghana and Togo. *PLoS. Negl. Trop. Dis.* 9, e3457 (2015).
79. Pan,H. et al. Ipr1 gene mediates innate immunity to tuberculosis. *Nature* 434, 767-772 (2005).
80. Dolganov,G.M. et al. A novel method of gene transcript profiling in airway biopsy homogenates reveals increased expression of a Na⁺-K⁺-Cl⁻ cotransporter (NKCC1) in asthmatic subjects. *Genome Res.* 11, 1473-1483 (2001).
81. Woodruff,P.G. et al. Genome-wide profiling identifies epithelial cell genes associated with asthma and with treatment response to corticosteroids. *Proc. Natl. Acad. Sci. U. S. A* 104, 15858-15863 (2007).

82. Yan, B.S. et al. Progression of pulmonary tuberculosis and efficiency of bacillus Calmette-Guerin vaccination are genetically controlled via a common sst1-mediated mechanism of innate immunity. *J. Immunol.* 179, 6919-6932 (2007).
83. Comas, I. et al. Human T cell epitopes of *Mycobacterium tuberculosis* are evolutionarily hyperconserved. *Nat. Genet.* 42, 498-503 (2010).
84. Krogh, A., Larsson, B., von, H.G., & Sonnhammer, E.L. Predicting transmembrane protein topology with a hidden Markov model: application to complete genomes. *J. Mol. Biol.* 305, 567-580 (2001).
85. Thomsen, M., Lundegaard, C., Buus, S., Lund, O., & Nielsen, M. MHCcluster, a method for functional clustering of MHC molecules. *Immunogenetics* 65, 655-665 (2013).
86. Franken, K.L. et al. Purification of his-tagged proteins by immobilized chelate affinity chromatography: the benefits from the use of organic solvent. *Protein Expr. Purif.* 18, 95-99 (2000).
87. Abdallah, A.M. et al. Type VII secretion—mycobacteria show the way. *Nat. Rev. Microbiol.* 5, 883-891 (2007).
88. Khadge, S. et al. Longitudinal immune profiles in type 1 leprosy reactions in Bangladesh, Brazil, Ethiopia and Nepal. *BMC. Infect. Dis.* 15, 477 (2015).

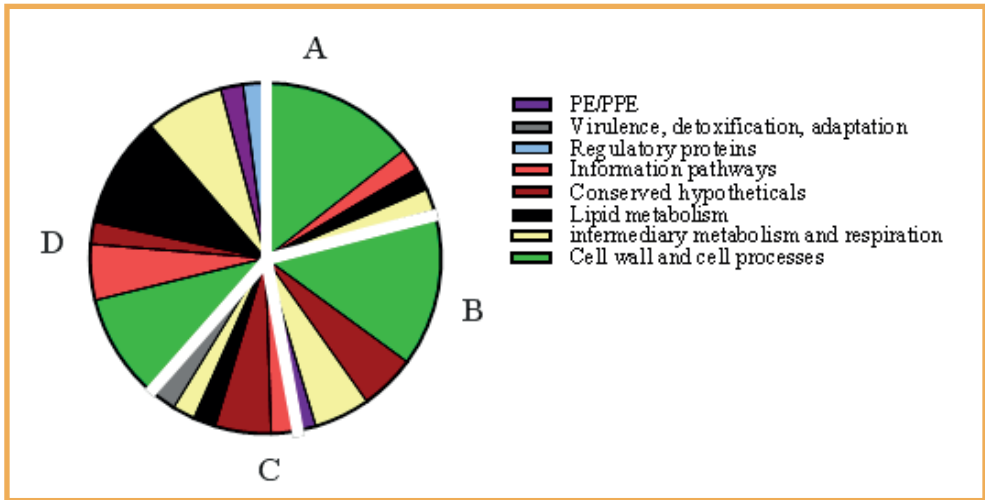
SUPPLEMENTARY INFORMATION



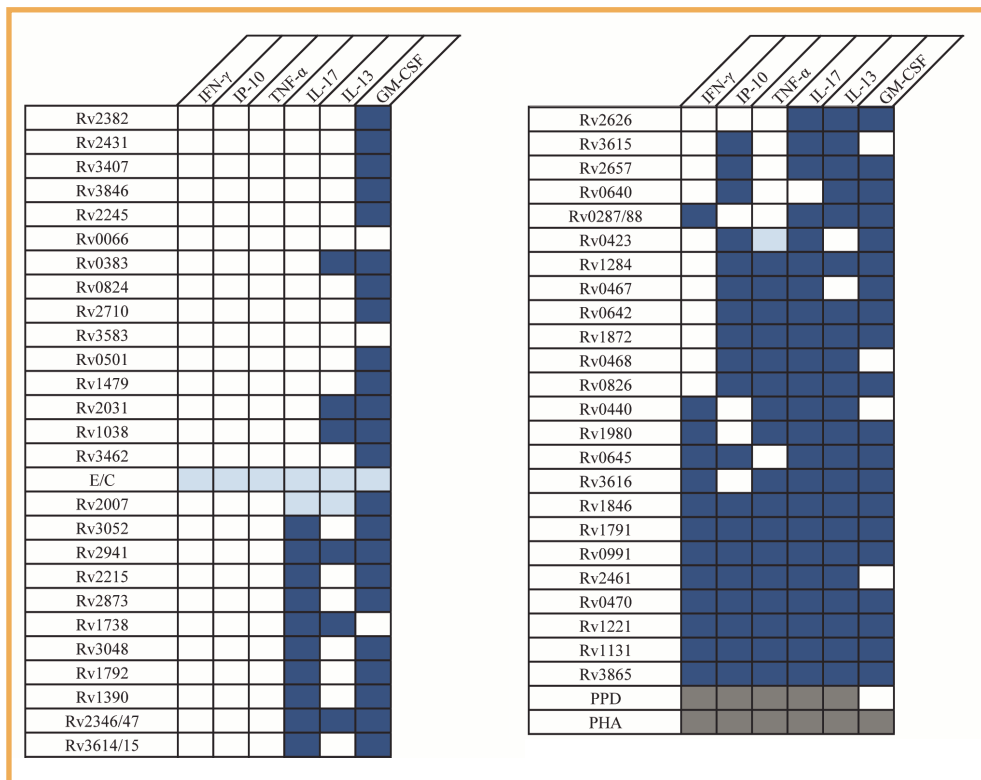
Supplementary Figure 1. Comparison of the functional classes of the top 15% up-regulated IVE-TB genes compared to the whole *Mtb* genome. The pie-charts (A) indicate the proportion of each functional category (as indicated in TubercuList) of the top 15% highly *in vivo* expressed *Mtb* (IVE-TB) genes ($n = 194$) and of the whole *Mtb* genome ($n = 4111$). The histogram (B) shows the ratio of the two proportions; ratios less or greater than 1 suggest the under- or over-representation of the indicated functional class in the top 15% IVE-TB genes, respectively.



Supplementary Figure 2. Immunodominance and immunogenicity of IVE-TB antigens based on cytokine production. PBMCs of *Mtb*-responders ($n =$ nine) were stimulated with IVE-TB antigens and tested for the level of multiple cytokines by multiplex assay. The frequency (x-axis) and the magnitude (y-axis) of responses were ranked to compare the immunodominance and the immunogenicity for each antigen per analyte as well as for positive controls (PPD and PHA). In quadrant A are the top antigens for immunogenicity, in quadrant C the top antigens for immunodominance, and in quadrant B the top antigens for both parameters. Results were compared by Spearman's rank correlation coefficient. Graphs are shown for IL-13 and GM-CSF.



Supplementary Figure 3. Functional classes of IVE-TB antigens recognised by latently *Mtb*-infected (LTBI) individuals. Functional categories (as described in TubercuList) are displayed for the IVE-TB antigens able to induce (A) four, (B) three, (C) two or (D) one cytokines in LTBI donors. The functional category of the *Mtb* protein does not correlate with the type of responses observed.



Supplementary Figure 4. E/C vs. IVE-TB antigens: comparison of the median cytokine fold-change of stimulated vs. unstimulated samples. Results based on multiplex assay performed with the supernatant of *Mtb*-exposed individuals ($n = 12$). Fold change similar to (■), greater than (■), or less than (□) that induced by E/C; (■): positive controls. E/C: ESAT6/CFP10.

Supplementary Table 1. List of the 194 highly expressed in-vivo *Mtb* (IVE-TB) genes identified in the lung of *Mtb* infected mice independently of their susceptibility to tuberculosis.

H37Rv identity	Described (predicted) function
Rv0046c	Myo-inositol-1-phosphate synthase Ino1
Rv0065	Possible toxin VapC1
Rv0066c	Probable isocitrate dehydrogenase [NADP] Icd2 (oxalosuccinate decarboxylase)
Rv0103c	Probable cation-transporter P-type ATPase B CtpB
Rv0140	Conserved protein
Rv0147	Probable aldehyde dehydrogenase (NAD+) dependent
Rv0188	Probable conserved transmembrane protein
Rv0206c	Possible conserved transmembrane transport protein MmpL3
Rv0211	iron-regulated phosphoenolpyruvate carboxykinase pckA
Rv0244c	Probable acyl-CoA dehydrogenase FadE5
Rv0249c	Probable succinate dehydrogenase
Rv0284	ESX conserved component EccC3.
Rv0287	Esat6 like protein esxG
Rv0288	Low molecular weight protein antigen 7 esxH
Rv0383c	Possible conserved secreted protein
Rv0423c	Probable thiamine biosynthesis protein ThiC
Rv0440	60 kDa chaperonin 2 GroEL2
Rv0451c	Probable conserved membrane protein MmpS4
Rv0453	PPE family protein PPE11
Rv0467	Isocitrate lyase Icl
Rv0468	3-hydroxybutyryl-CoA dehydrogenase FadB2
Rv0469	Possible mycolic acid synthase UmaA
Rv0470c	Mycolic acid synthase PcaA
Rv0474	Probable transcriptional regulatory protein
Rv0476	Possible conserved transmembrane protein
Rv0501	Possible UDP-glucose 4-epimerase GalE2
Rv0572c	Hypothetical protein
Rv0638	Probable preprotein translocase SecE1
Rv0640	50S ribosomal protein L11 RplK
Rv0642c	Methoxy mycolic acid synthase 4 MmaA4
Rv0645c	Methoxy mycolic acid synthase 1 MmaA1
Rv0711	Possible arylsulfatase AtsA
Rv0715	50S ribosomal protein L24 RplX
Rv0717	30S ribosomal protein S14 RpsN1

Rv0759c	Conserved hypothetical protein
Rv0761c	Possible zinc-containing alcohol dehydrogenase NAD dependent AdhB
Rv0805	Class III cyclic nucleotide phosphodiesterase
Rv0815c	Probable thiosulfate sulfurtransferase CysA2
Rv0824c	Probable acyl-[acyl-carrier protein] desaturase DesA1
Rv0826	Conserved hypothetical protein
Rv0884c	Possible phosphoserine aminotransferase SerC
Rv0932c	Periplasmic phosphate-binding lipoprotein PstS2
Rv0951	Probable succinyl-CoA synthetase
Rv0986	Probable adhesion component transport ATP-binding protein ABC transporter
Rv0991	Conserved serine rich protein
Rv1013	Putative polyketide synthase Pks16
Rv1037c	Putative ESAT6 like protein EsxI
Rv1038c	Esat6 like protein esxJ
Rv1093	Serine hydroxymethyltransferase 1 GlyA1
Rv1109c	Conserved protein
Rv1131	Probable methylcitrate synthase PrpC
Rv1156	Conserved protein
Rv1174c	Low molecular weight T-cell antigen TB8.4
Rv1182	Probable conserved polyketide synthase associated protein PapA3
Rv1194c	Conserved protein
Rv1197	ESAT6 like protein EsxK
Rv1221	Alternative RNA polymerase sigma factor sigE
Rv1248c	Multifunctional alpha-ketoglutarate metabolic enzyme
Rv1270c	Possible lipoprotein LprA
Rv1274	Possible lipoprotein LprB
Rv1284	Beta-carbonic anhydrase
Rv1286	Probable bifunctional enzyme CysN/CysC
Rv1297	Probable transcription termination factor Rho homolog
Rv1298	50S ribosomal protein L31 RpmE
Rv1303	Conserved hypothetical transmembrane protein
Rv1304	Probable ATP synthase a chain AtpB
Rv1305	Probable ATP synthase C chain AtpE
Rv1308	Probable ATP synthase alpha chain AtpA
Rv1324	Possible thioredoxin
Rv1331	Conserved hypothetical protein
Rv1335	Sulfur carrier protein CysO
Rv1388	Putative integration host factor MihF

Rv1390	Probable DNA-directed RNA polymerase
Rv1398	Possible antitoxin VapB10
Rv1404	Probable transcriptional regulatory protein
Rv1411c	Conserved lipoprotein LprG
Rv1419	Unknown protein
Rv1440	Probable protein-export membrane protein
Rv1449c	Transketolase Tkt
Rv1467c	Probable acyl-CoA dehydrogenase FadE15
Rv1471	Probable thioredoxin TrxB1
Rv1479	Probable transcriptional regulatory protein MoxR1
Rv1611	Probable indole-3-glycerol phosphate synthase TrpC
Rv1630	30S ribosomal protein S1 RpsA
Rv1636	Iron-regulated universal stress protein family protein TB15.3
Rv1641	Probable initiation factor if-3 InfC
Rv1738	Conserved hypothetical protein
Rv1783	ESX conserved component EccC5
Rv1784	Conserved hypothetical protein
Rv1791	PE family protein PE19
Rv1792	ESAT6 like protein EsxM
Rv1793	Putative ESAT6 like protein EsxN
Rv1794	Conserved protein
Rv1795	ESX conserved component EccD5
Rv1805c	Hypothetical protein
Rv1829	Conserved protein
Rv1831	Hypothetical protein
Rv1846c	Transcriptional repressor Blal
Rv1854c	Probable NADH dehydrogenase Ndh
Rv1872c	Possible L-lactate dehydrogenase
Rv1876	Probable bacterioferritin BfrA
Rv1880c	Probable cytochrome P450 140 Cyp140
Rv1888c	Possible transmembrane protein
Rv1909c	Ferric uptake regulation protein FurA
Rv1915	Probable isocitrate lyase AceAa
Rv1925	Probable acyl-CoA ligase FadD31
Rv1980c	Immunogenic protein Mpt64
Rv1981c	Ribonucleoside-diphosphate reductase
Rv1984c	Probable cutinase precursor CFP21
Rv2007	Ferredoxin fdxA

Rv2031	Heat shock protein hspX
Rv2091c	Probable membrane protein
Rv2108	PPE family protein PPE36
Rv2115c	Mycobacterial proteasome ATPase Mpa
Rv2193	Probable cytochrome C oxidase (subunit III) CtaE
Rv2194	Probable ubiquinol-cytochrome C reductase QcrC
Rv2215	DlaT, dihydrolipoamide acyltransferase, E2 component of pyruvate dehydrogenase
Rv2219	Probable conserved transmembrane protein
Rv2245	3-oxoacyl-[acyl-carrier protein] synthase 1 KasA
Rv2334	Cysteine synthase a CysK1
Rv2346c	Putative ESAT6 like protein EsxO
Rv2347c	Putative ESAT6 like protein EsxP
Rv2382	Polyketide synthetase mbtC
Rv2389c	Probable resuscitation-promoting factor RpfD
Rv2428	Alkyl hydroperoxide reductase C protein AhpC
Rv2431c	PE family protein PE25
Rv2455c	Probable oxidoreductase
Rv2457c	Probable ATP-dependent CLP protease ATP-binding subunit ClpX
Rv2460c	Probable ATP-dependent CLP protease proteolytic subunit 2 ClpP2
Rv2461c	Probable ATP-dependent CLP protease proteolytic subunit 1 ClpP1
Rv2582	Probable peptidyl-prolyl cis-trans isomerase B PpiB
Rv2617c	Probable transmembrane protein
Rv2626	Hypoxic response protein 1 Hrp1
Rv2657c	Probable PhiRv2 prophage protein
Rv2663	Hypothetical protein
Rv2699c	Conserved hypothetical protein
Rv2710	RNA polymerase sigma factor sigB
Rv2716	Conserved protein
Rv2873	Cell surface lipoprotein Mpt83
Rv2875	Major secreted immunogenic protein Mpt70
Rv2876	Possible conserved transmembrane protein
Rv2878c	Soluble secreted antigen Mpt53 precursor
Rv2882c	Ribosome recycling factor Frr
Rv2890c	30S ribosomal protein S2 RpsB
Rv2931	Phenolphthiocerol synthesis type-I polyketide synthase PpsA
Rv2932	Phenolphthiocerol synthesis type-I polyketide synthase PpsB
Rv2934	Phenolphthiocerol synthesis type-I polyketide synthase PpsD
Rv2935	Phenolphthiocerol synthesis type-I polyketide synthase PpsE

Rv2936	Daunorubicin-dim-transport ATP-binding protein ABC transporter DrrA
Rv2939	Possible conserved polyketide synthase associated protein PapA5
Rv2941	Fatty-acid-AMP ligase FadD28
Rv3048c	Ribonucleoside-diphosphate reductase
Rv3051c	Ribonucleoside-diphosphate reductase NrdE (R1F protein)
Rv3052	hypothetical protein nrdI
Rv3141	Probable NADPH quinone oxidoreductase FadB4
Rv3193c	Probable conserved transmembrane protein
Rv3213c	Possible SOJ/para-related protein
Rv3219	Transcriptional regulator whib-like whiB1
Rv3246c	Two component sensory transduction transcriptional regulatory protein MtrA
Rv3248c	Probable adenosylhomocysteinase SahH
Rv3280	Probable propionyl-CoA carboxylase beta chain 5 AccD5
Rv3407	Possible antitoxin VapB47
Rv3416	Transcriptional regulatory protein WhiB-like WhiB3
Rv3418c	10 kDa chaperonin GroES
Rv3460c	30S ribosomal protein S13 RpsM
Rv3462	Translation initiation factor IF-1 infA
Rv3528c	Unknown protein
Rv3583c	Possible transcription factor
Rv3596c	Probable ATP-dependent protease ATP-binding subunit ClpC1
Rv3601c	Probable aspartate 1-decarboxylase precursor PanD
Rv3614c	ESX-1 secretion-associated protein EspD
Rv3615	ESX-1 secretion-associated protein EspC
Rv3616	Conserved alanine and glycine rich protein
Rv3619c	Putative ESAT6 like protein EsxV
Rv3620c	Putative ESAT6 like protein EsxW
Rv3667	Acetyl-coenzyme A synthetase Acs
Rv3681c	Probable transcriptional regulatory protein WhiB-like WhiB4
Rv3682	Probable bifunctional membrane-associated penicillin-binding protein 1A/1B PonA2
Rv3824c	Conserved polyketide synthase associated protein PapA1
Rv3841	Bacterioferritin BfrB
Rv3846	Superoxide dismutase sodA
Rv3854c	Monoxygenase EthA
Rv3857c	Possible membrane protein
Rv3858c	Probable NADH-dependent glutamate synthase
Rv3863	Unknown alanine rich protein
Rv3864	ESX-1 secretion-associated protein EspE

Rv3865	ESX-1 secretion-associated protein EspF
Rv3874	10 kDa culture filtrate antigen EsxB (LHP) (CFP10)
Rv3875	6 kda early secretory antigenic target esxA
Rv3878	ESX-1 secretion-associated protein EspJ
Rv3879c	ESX-1 secretion-associated protein EspK
Rv3881c	Secreted ESX-1 substrate protein B, EspB
Rv3890c	ESAT6 like protein EsxC
Rv3914	Thioredoxin trxC

